

International Journal of Modern Physics E
 © World Scientific Publishing Company

CONSTITUENT QUARK MODEL DESCRIPTION OF CHARMONIUM PHENOMENOLOGY

J. SEGOVIA

*Physics Division, Argonne National Laboratory, 9700 South Cass Avenue
 Argonne, Illinois 60439-4832, United States of America
 jsegovia@anl.gov*

D.R. ENTEM

*Grupo de Física Nuclear e Instituto Universitario de Física Fundamental y Matemáticas,
 Universidad de Salamanca, Casas del Parque S/N
 Salamanca, E-37008, Spain
 entem@usal.es*

F. FERNANDEZ

*Grupo de Física Nuclear e Instituto Universitario de Física Fundamental y Matemáticas,
 Universidad de Salamanca, Casas del Parque S/N
 Salamanca, E-37008, Spain
 fdz@usal.es*

E. HERNANDEZ

*Grupo de Física Nuclear e Instituto Universitario de Física Fundamental y Matemáticas,
 Universidad de Salamanca, Plaza de la Merced S/N
 Salamanca, E-37008, Spain
 gajatee@usal.es*

Received February 26, 2022

We review the ability of the quark models to describe the phenomenology of the charm meson sector. The spectroscopy and decays of charmonium and open charm mesons are described in a particular quark model and compared with the data and the results of other models existing in the literature. A quite reasonable global description of the heavy meson spectra is reached. A new assignment of the $\psi(4415)$ resonance as a $3D$ state leaving aside the $4S$ state to the $X(4360)$ is tested through the analysis of the resonance structure in e^+e^- exclusive reactions around the $\psi(4415)$ energy region. We make tentative assignments of some of the XYZ mesons.

To elucidate the structure of the $1^+ c\bar{s}$ states, i.e. $D_{s1}(2460)$ and $D_{s1}(2536)$, we study the strong decay properties of the $D_{s1}(2536)$ meson. We also perform a calculation of the branching fractions for the semileptonic decays of B and B_s mesons into final states containing orbitally excited charmed and charmed-strange mesons, which have become a very important source of information about the structure of heavy mesons. Analysis of the nonleptonic B meson decays into $D^{(*)}D_{sJ}$ are also included.

Keywords: potential models; Heavy quarkonia; charmed mesons; bottom mesons; models

2 *J. Segovia, D.R. Entem, F. Fernandez and E. Hernandez*

of strong interactions; leptonic and semileptonic decays.

12.39.Pn, 14.40.Pq, 14.40.Nd, 14.40.Lb, 12.40.-y, 13.20.-v

1. Introduction

After the November revolution in 1974, the next significant step in the understanding of charmonium physics was the starting of the experimental activity at the dawn of the XXI century of the B-factories and the advent of the LHCb.

These machines have produced a huge amount of data which will allow a better understanding of the quarkonium phenomenology. Reviews of the theoretical importance and experimental status of heavy quarkonium have recently been given, among others, by Quigg,¹ Galik,² the CERN Quarkonium Working Group,³ Seth,⁴⁻⁶ and Swarnicki.⁷

Although the spectrum of charmonium and their transitions have been the subject of a great number of studies, from the seminal paper of Eichten⁸ to the more recent results presented by Radford and Repko,⁹ there are only few global studies of all the data produced at the B factories. As most of the new states lie above the open charm threshold, the study of its decay properties through the $D^{(*)}\bar{D}^{(*)}$ channels are very important. This implies a consistent description of both, the parent meson and the $D^{(*)}$ mesons involved in the decay. Furthermore, most of the new resonances are produced through a weak process, so that a wealth of information about the new states can be obtained from the study of the weak decay of B mesons.

All these processes have been partially studied in the literature but the aim of this review is to present a coherent description of as many experimental data as possible in an unique framework. We will provide the comparison with the results of other models where there exist.

With this idea, after a short introduction to the model used, we will describe the spectroscopy of the hidden and open charm mesons as $q\bar{q}$ states, discussing whose of the new XYZ states can be assigned to this structure. The description of theses states will be complemented with the study of the electromagnetic and strong decays.

One of the outcoming of our calculation is a new quantum number assignment of the $\psi(4415)$ state motivated by the appearance in the $J^{PC} = 1^{--}$ spectrum of the $X(4360)$ state. A detailed study of the reactions $e^+e^- \rightarrow D^0 D^- \pi^+$ and $e^+e^- \rightarrow D^0 D^{*-} \pi^+$ has been performed in order to justify our result.

In the same way, a study of the decay properties of the $D_{s1}(2536)^+$ meson has been performed and compare with the data of the BELLE collaboration to give more insight in the structure of the $1^+ c\bar{s}$ states.

Finally, most of the new states have been discovered from the semileptonic and non-leptonic B decays into open charm states. The theoretical analysis of the data, which includes both weak and strong processes, opens an interesting possibility to study the structure of this type of mesons.

The paper is organized as follows. In Sec. 2 we will introduce our constituent quark model, paying special attention to the terms that determine the spectra of heavy mesons. After that, we will present in Sec. 3 the spectrum of hidden-charm and open charm mesons and its electromagnetic decays. Sec. 4 is devoted to the study of strong decays and reactions, whereas in Sec. 6, we perform the study of the B weak decays into open charm states. We end by summarizing the work and giving some conclusions in Sec. 7.

2. Constituent Quark Model

Constituent quark models have a long history starting from the Isgur seminal work (see, for example Refs. 10 and 11) in which the potential between two massive quarks (constituents) was modeled by a quadratic confinement potential plus a chromomagnetic interaction. This model was successful in explaining the baryon and meson spectra known at that time. In the eighties it was realized that the constituent mass is a consequence of the chiral symmetry breaking in the light quark sector at a momentum scale Λ_{sb} greater than the confinement scale Λ_{conf} .¹² In the region between the two scales, due to this breaking, the quark propagator gets modified and quarks acquire a dynamical momentum dependent mass.¹³ The Lagrangian describing this scenario must contain chiral fields to compensate the mass term. The Goldstone bosons associated to the chiral fields leads to an additional interaction between light quarks. This fact does not affect to the heavy quark sector but is of paramount importance in the molecular picture because the only remaining interaction between the two molecular components, due to its color singlet nature, is the one driven by the Goldstone boson exchanges between the light quarks.

The simplest Lagrangian which contains chiral fields to compensate the mass term can be expressed as

$$\mathcal{L} = \bar{\psi}(i\not{\partial} - M(q^2)U^{\gamma_5})\psi \quad (1)$$

where $U^{\gamma_5} = \exp(i\pi^a\lambda^a\gamma_5/f_\pi)$, π^a denotes nine pseudoscalar fields ($\eta_0, \vec{\pi}, K_i, \eta_8$) with $i=1, \dots, 4$ and $M(q^2)$ is the constituent mass. This constituent quark mass, which vanishes at large momenta and is frozen at low momenta at a value around 300 MeV, can be explicitly obtained from the theory but its theoretical behavior can be simulated by parametrizing $M(q^2) = m_q F(q^2)$ where $m_q \simeq 300$ MeV, and

$$F(q^2) = \left[\frac{\Lambda^2}{\Lambda^2 + q^2} \right]^{\frac{1}{2}}. \quad (2)$$

The cut-off Λ fixes the chiral symmetry breaking scale.

The Goldstone boson field matrix U^{γ_5} can be expanded in terms of boson fields,

$$U^{\gamma_5} = 1 + \frac{i}{f_\pi}\gamma_5\lambda^a\pi^a - \frac{1}{2f_\pi^2}\pi^a\pi^a + \dots \quad (3)$$

4 *J. Segovia, D.R. Entem, F. Fernandez and E. Hernandez*

The first term of the expansion generates the constituent quark mass, while the second gives rise to a one-boson exchange interaction between quarks. The main contribution of the third term comes from the two-pion exchange which has been simulated by means of a scalar exchange potential.

In the heavy quark sector chiral symmetry is explicitly broken and this type of interaction does not act. However it constrains the model parameters through the light meson phenomenology and provides a natural way to incorporate the pion exchange interaction in the molecular dynamics.

Beyond the chiral symmetry breaking scale one expects the dynamics to be governed by QCD perturbative effects. They are taken into account through the one gluon-exchange interaction.

The one-gluon exchange potential is generated from the vertex Lagrangian

$$\mathcal{L}_{q\bar{q}g} = i\sqrt{4\pi\alpha_s}\bar{\psi}\gamma_\mu G_c^\mu \lambda^c \psi, \quad (4)$$

where λ^c are the $SU(3)$ color matrices and G_c^μ is the gluon field. The resulting potential contains central, tensor and spin-orbit contributions given by

$$\begin{aligned} V_{\text{OGE}}^{\text{C}}(\vec{r}_{ij}) &= \frac{1}{4}\alpha_s(\vec{\lambda}_i^c \cdot \vec{\lambda}_j^c) \left[\frac{1}{r_{ij}} - \frac{1}{6m_i m_j}(\vec{\sigma}_i \cdot \vec{\sigma}_j) \frac{e^{-r_{ij}/r_0(\mu)}}{r_{ij}r_0^2(\mu)} \right], \\ V_{\text{OGE}}^{\text{T}}(\vec{r}_{ij}) &= -\frac{1}{16}\frac{\alpha_s}{m_i m_j}(\vec{\lambda}_i^c \cdot \vec{\lambda}_j^c) \left[\frac{1}{r_{ij}^3} - \frac{e^{-r_{ij}/r_g(\mu)}}{r_{ij}} \left(\frac{1}{r_{ij}^2} + \frac{1}{3r_g^2(\mu)} + \frac{1}{r_{ij}r_g(\mu)} \right) \right] S_{ij}, \\ V_{\text{OGE}}^{\text{SO}}(\vec{r}_{ij}) &= -\frac{1}{16}\frac{\alpha_s}{m_i^2 m_j^2}(\vec{\lambda}_i^c \cdot \vec{\lambda}_j^c) \left[\frac{1}{r_{ij}^3} - \frac{e^{-r_{ij}/r_g(\mu)}}{r_{ij}^3} \left(1 + \frac{r_{ij}}{r_g(\mu)} \right) \right] \times \\ &\quad \times \left[((m_i + m_j)^2 + 2m_i m_j)(\vec{S}_+ \cdot \vec{L}) + (m_j^2 - m_i^2)(\vec{S}_- \cdot \vec{L}) \right], \end{aligned} \quad (5)$$

where $r_0(\mu_{ij}) = \hat{r}_0 \frac{\mu_{nn}}{\mu_{ij}}$ and $r_g(\mu_{ij}) = \hat{r}_g \frac{\mu_{nn}}{\mu_{ij}}$ are regulators. Note that the contact term of the central part of the one-gluon exchange potential has been regularized as follows

$$\delta(\vec{r}_{ij}) \sim \frac{1}{4\pi r_0^2} \frac{e^{-r_{ij}/r_0}}{r_{ij}}. \quad (6)$$

To improve the description of mesons with different flavored quarks we include

one-loop corrections to the OGE potential as derived by Gupta *et al.*¹⁴

$$\begin{aligned}
V_{\text{OGE}}^{1\text{-loop,C}}(\vec{r}_{ij}) &= 0, \\
V_{\text{OGE}}^{1\text{-loop,T}}(\vec{r}_{ij}) &= \frac{C_F}{4\pi} \frac{\alpha_s^2}{m_i m_j} \frac{1}{r^3} S_{ij} \left[\frac{b_0}{2} \left(\ln(\mu r_{ij}) + \gamma_E - \frac{4}{3} \right) + \frac{5}{12} b_0 - \frac{2}{3} C_A \right. \\
&\quad \left. + \frac{1}{2} \left(C_A + 2C_F - 2C_A \left(\ln(\sqrt{m_i m_j} r_{ij}) + \gamma_E - \frac{4}{3} \right) \right) \right], \\
V_{\text{OGE}}^{1\text{-loop,SO}}(\vec{r}_{ij}) &= \frac{C_F}{4\pi} \frac{\alpha_s^2}{m_i^2 m_j^2} \frac{1}{r^3} \times \\
&\times \left\{ (\vec{S}_+ \cdot \vec{L}) \left[((m_i + m_j)^2 + 2m_i m_j) (C_F + C_A - C_A (\ln(\sqrt{m_i m_j} r_{ij}) + \gamma_E)) \right. \right. \\
&\quad \left. \left. + 4m_i m_j \left(\frac{b_0}{2} (\ln(\mu r_{ij}) + \gamma_E) - \frac{1}{12} b_0 - \frac{1}{2} C_F - \frac{7}{6} C_A + \frac{C_A}{2} (\ln(\sqrt{m_i m_j} r_{ij}) + \gamma_E) \right) \right. \right. \\
&\quad \left. \left. + \frac{1}{2} (m_j^2 - m_i^2) C_A \ln \left(\frac{m_j}{m_i} \right) \right] \right. \\
&\quad \left. + (\vec{S}_- \cdot \vec{L}) \left[(m_j^2 - m_i^2) (C_F + C_A - C_A (\ln(\sqrt{m_i m_j} r_{ij}) + \gamma_E)) \right. \right. \\
&\quad \left. \left. + \frac{1}{2} (m_i + m_j)^2 C_A \ln \left(\frac{m_j}{m_i} \right) \right] \right\}, \tag{7}
\end{aligned}$$

where $C_F = 4/3$, $C_A = 3$, $b_0 = 9$, $\gamma_E = 0.5772$ and the scale $\mu \sim 1 \text{ GeV}$.

Although there is no analytical proof, it is a general belief that confinement emerges from the force between the gluon color charges. When two quarks are separated, due to the non-Abelian character of the theory, the gluon fields self-interact forming color strings which bring the quarks together.

In a pure gluon gauge theory the potential energy of the $q\bar{q}$ pair grows linearly with the quark-antiquark distance. However, in full QCD the presence of sea quarks may soften the linear potential, due to the screening of the color charges, and eventually leads to the breaking of the string. This characteristic can be translated into a screened potential in such a way that the potential saturates at the same interquark distance.

$$\begin{aligned}
V_{\text{CON}}^{\text{C}}(\vec{r}_{ij}) &= [-a_c(1 - e^{-\mu_c r_{ij}}) + \Delta] (\vec{\lambda}_i^c \cdot \vec{\lambda}_j^c), \\
V_{\text{CON}}^{\text{SO}}(\vec{r}_{ij}) &= -(\vec{\lambda}_i^c \cdot \vec{\lambda}_j^c) \frac{a_c \mu_c e^{-\mu_c r_{ij}}}{4m_i^2 m_j^2 r_{ij}} \times \\
&\times \left[((m_i^2 + m_j^2)(1 - 2a_s) + 4m_i m_j(1 - a_s))(\vec{S}_+ \cdot \vec{L}) \right. \\
&\quad \left. + (m_j^2 - m_i^2)(1 - 2a_s)(\vec{S}_- \cdot \vec{L}) \right], \tag{8}
\end{aligned}$$

where a_s controls the mixture between the scalar and vector Lorentz structures of the confinement. At short distances this potential presents a linear behavior with

an effective confinement strength, $\sigma = -a_c \mu_c (\vec{\lambda}_i^c \cdot \vec{\lambda}_j^c)$, while it becomes constant at large distances. This type of potential shows a threshold defined by

$$V_{\text{thr}} = \{-a_c + \Delta\}(\vec{\lambda}_i^c \cdot \vec{\lambda}_j^c). \quad (9)$$

No $q\bar{q}$ bound states can be found for energies higher than this threshold. The system suffers a transition from a color string configuration between two static color sources into a pair of static mesons due to the breaking of the color string and the most favored decay into hadrons.

Among the different methods to solve the Schrödinger equation and find the quark-antiquark bound states, we use the Gaussian Expansion Method¹⁵ because it provides enough accuracy and it makes the subsequent evaluation of the decay amplitude matrix elements easier.

This procedure provides the radial wave function solution of the Schrödinger equation as an expansion in terms of basis functions

$$R_\alpha(r) = \sum_{n=1}^{n_{max}} c_n^\alpha \phi_{nl}^G(r), \quad (10)$$

where α refers to the channel quantum numbers. The coefficients, c_n^α , and the eigenvalue, E , are determined from the Rayleigh-Ritz variational principle

$$\sum_{n=1}^{n_{max}} \left[(T_{n'n}^\alpha - E N_{n'n}^\alpha) c_n^\alpha + \sum_{\alpha'} V_{n'n}^{\alpha\alpha'} c_n^{\alpha'} = 0 \right], \quad (11)$$

where $T_{n'n}^\alpha$, $N_{n'n}^\alpha$ and $V_{n'n}^{\alpha\alpha'}$ are the matrix elements of the kinetic energy, the normalization and the potential, respectively. $T_{n'n}^\alpha$ and $N_{n'n}^\alpha$ are diagonal whereas the mixing between different channels is given by $V_{n'n}^{\alpha\alpha'}$.

Following Ref. 15, we employ Gaussian trial functions with ranges in geometric progression. This enables the optimization of ranges employing a small number of free parameters. Moreover, the geometric progression is dense at short distances, so that it allows the description of the dynamics mediated by short range potentials. The fast damping of the gaussian tail is not a problem, since we can choose the maximal range much longer than the hadronic size.

Table 1 shows the model parameters fitted over all meson spectra and relevant for the heavy quark sectors, which have been taken from Ref. 16.

Table 1. Model parameters fitted over all meson spectra and relevant for the heavy quark sectors.

Quark masses	m_n (MeV)	313
	m_s (MeV)	555
	m_c (MeV)	1763
	m_b (MeV)	5110
OGE	α_0	2.118
	Λ_0 (fm $^{-1}$)	0.113
	μ_0 (MeV)	36.976
	\hat{r}_0 (fm)	0.181
	\hat{r}_g (fm)	0.259
Confinement	a_c (MeV)	507.4
	μ_c (fm $^{-1}$)	0.576
	Δ (MeV)	184.432
	a_s	0.81

3. Spectroscopy

3.1. Charmonium

Shortly after the discovery by BELLE of the missing $\eta'_c(2^1S_0)$,²⁵ new states containing charm quarks have appeared in great profusion. Some of them have been identified as canonical $c\bar{c}$ states. but others, called collectively as XYZ states, exhibit unexpected properties which hardly fit with those of two quark states.

The charmonium spectrum is given in Table 2. We compare our results with the experimental data and with those predicted by other significant quark models in the literature: S. Godfrey and N. Isgur;¹⁸ and D. Ebert, R.N. Faustov and V.O. Galkin.¹⁹ Some tentative XYZ assignments attending to the masses have been done. The experimental masses are taken from Particle Data Group (PDG)¹⁷ for the well established states and from their respective original works for XYZ mesons.

As one can see in Table 2, we obtain a quite reasonable global description of the charmonium sector. This feature is also reached by other quark models. The spectrum predicted by the different models is quite similar at least for the low lying levels. However, while our confining term is based on a screened linear potential at large interquark distances, the remaining models implement a linear potential for all distances. This can be translated into a different prediction of the masses for the higher excited states, the screened linear potential reduces the masses of higher excited states, see Table 2. This has an important consequence, the new assignment of the $\psi(4415)$. Usually this state has been assigned as a $4S$ state. Our particular choice of the potential includes the new $X(4360)$ as a $4S$ state between the well established $\psi(4160)$ and $\psi(4415)$ which are both predicted as D -wave

states. Moreover we can assign as $1^{--} c\bar{c}$ structures the new $X(4630)$ and $X(4660)$ mesons whose nature is still unclear.

It is important to remark that a nonrelativistic treatment of the quark-antiquark system is performed in our approach. However, a relativistic scheme is used for the quark models of Refs. 18 and 19. The relativistic effects should be small due to the large mass of the c -quark. Therefore, the differences on the spectrum between both schemes are negligible and can be absorbed in the reparametrization of the model.

The $\eta_c(1S)$ is the lowest state of charmonium. The model predicts a mass of 2990 MeV, in good agreement with the experimental one. The splitting between 1^1S_0 and 1^3S_1 is given by the Dirac delta term of the OGE potential. This splitting is measured experimentally to be 116.6 ± 1.2 MeV which is in reasonable agreement with our prediction of 106 MeV. Moreover, our predicted mass for the $\eta_c(2S)$ is 3643 MeV, which agrees with the experimental value.

Lattice data show a vanishing long-range component of the spin-spin potential. Thus, this part of the potential appears to be entirely dominated by its short-range, delta-like term, suggesting that the 1P_1 should be close to the center-of-gravity of the 3P_J system. The precision measurement of the $h_c(1P)$ mass was reported by CLEO in 2008,²⁶ $3525.28 \pm 0.19 \pm 0.12$ MeV. Later, BES III²⁷ has confirmed this with a mass of $3525.40 \pm 0.13 \pm 0.18$ MeV. The centroid of the 1^3P_J states is known to be 3525.30 ± 0.04 MeV¹⁷ and then the hyperfine splitting is $+0.02 \pm 0.23$ MeV from CLEO and -0.10 ± 0.22 MeV from BES III. The comparison in our model between the centroid of 3P_J states and the corresponding h_c mass shows that our spin-spin interaction is negligible for these channels and it is in perfect agreement with the lattice expectations and the experimental measurements for the ground state.

As shown in Table 2 the long known 1^3P_J states are in agreement with the model results. The mean $2P$ multiplet mass is predicted to be near 3.95 GeV. Although no $2P c\bar{c}$ state has been clearly seen experimentally, there are reports from the different Collaborations which claim enhancements in that energy region. Among them one can cite the $X(3872)$, $X(3915)$, $Y(3940)$, $X(3940)$ and $Z(3930)$.

The $X(3872)$ mass is difficult to reproduce by the standard quark models, see Table 2. The $X(3872)$ mass is extremely close to the $D^0 D^{*0}$ threshold so it appears as a natural candidate to an even C -parity $D^0 D^{*0}$ molecule. The molecular interpretation will also explain the large isospin violation, but runs into trouble when it tries to explain the high $\gamma\psi'$ decay rate. This puzzling situation suggests for the $X(3872)$ state a combination of a $2P c\bar{c}$ state and a weakly-bound $D^0 D^{*0}$ molecule. In Ref. 28 we have performed a coupled channel calculation of the $1^{++} c\bar{c}$ sector including $q\bar{q}$ and $q\bar{q}q\bar{q}$ configurations. Two and four quark configurations are coupled nonperturbatively using the 3P_0 model. The elusive $X(3872)$ meson appears as a new state with a high probability for the DD^* molecular component. The original $c\bar{c}(2^3P_1)$ state acquires a sizable DD^* component and can be identified with the $X(3940)$.

The $Y(3940) \rightarrow \omega J/\psi$ enhancement was initially found by Belle²⁹ in $B^+ \rightarrow K^+ Y(3940)$ decays. It was confirmed by BaBar³⁰ with more statistics, albeit with somewhat smaller mass. But Belle²⁰ also found a statistically compelling resonant structure $X(3915)$ in $\gamma\gamma$ fusion decaying to $\omega J/\psi$. It shares the same production and decay signature as that of BaBar's $Y(3940)$, which has mass and width consistent with the $X(3915)$. An interpretation of these two states as been the same appears as a widely accepted idea and the name which is conserved is $X(3915)$. We only know at the moment that this state has an even C -parity. If $X(3915)$ was a $c\bar{c}$ state, the most probable quantum numbers would be 0^{++} . The mass predicted for the 2^3P_0 is 3909, in very good agreement with the experimental measurement.

In 2005 Belle²³ observed an enhancement in the $D\bar{D}$ mass spectrum from $e^+e^- \rightarrow e^+e^- D\bar{D}$ events with a statistical significance of 5.3σ . It was initially dubbed the $Z(3930)$, but since then it has been widely (if not universally) accepted as the $\chi_{c2}(2P)$. There is some Lattice calculations³¹ which suggest that the $\chi_{c2}(2P)$ and the 1^3F_2 state could be quite close in mass, so that perhaps the $Z(3930)$ is not the 2^3P_2 but rather the 1^3F_2 . Table 2 shows that all quark models predict a mass splitting between both states of about tens of MeV, so we do not consider that those states are nearby degenerated and assign the $Z(3930)$ as the 2^3P_2 state.

The Belle Collaboration has recently reported measurements of $B \rightarrow \chi_{c1}\gamma K$ and $\chi_{c2}\gamma K$.²⁴ They found evidence of a new resonance in the $\chi_{c1}\gamma$ final state with a mass of $(3823.1 \pm 1.8 \pm 0.7)$ MeV, a value which is consistent with the 1^3D_2 $c\bar{c}$ state according to our model, 3812 MeV. We expect that the 1^1D_2 state appears in the same energy range of the $X(3823)$, however, as we will see below, this state should appear in the $h_c\gamma$ channel.

Table 2. Masses, in MeV, of charmonium states. Some tentative XYZ assignments attending to the masses have been done. The experimental masses are taken from Particle Data Group (PDG)¹⁷ for the well established states and from their respective original works for XYZ mesons. We compare our results (labeled as The.) with those predicted by other significant quark models in the literature: S. Godfrey and N. Isgur;¹⁸ and D. Ebert, R.N. Faustov and V.O. Galkin.¹⁹

Ref.	Assignment	J^{PC}	nL	The.	Ref. 18	Ref. 19	Exp.
17	$\eta_c(1S)$	0^{-+}	$1S$	2990	2970	2981	2981.0 ± 1.1
17	$\eta_c(2S)$		$2S$	3643	3620	3635	3638.9 ± 1.3
			$3S$	4054	4060	3989	-
17	$\chi_{c0}(1P)$	0^{++}	$1P$	3452	3440	3413	3414.75 ± 0.31
20	$X(3915)$		$2P$	3909	3920	3870	$3915 \pm 3 \pm 2$
			$3P$	4242	-	4301	-
17	$h_c(1P)$	1^{+-}	$1P$	3515	3520	3525	3525.41 ± 0.16
			$2P$	3956	3960	3926	-
			$3P$	4278	-	4337	-
17	J/ψ	1^{--}	$1S$	3096	3100	3096	3096.916 ± 0.011
17	$\psi(2S)$		$2S$	3703	3680	3685	3686.108 ± 0.018
17	$\psi(3770)$		$1D$	3796	3820	3783	3778.1 ± 1.2
17	$\psi(4040)$		$3S$	4097	4100	4039	4039 ± 1
17	$\psi(4160)$		$2D$	4153	4190	4150	4153 ± 3
21	$X(4360)$		$4S$	4389	4450	4427	$4361 \pm 9 \pm 9$
17	$\psi(4415)$		$3D$	4426	4520	4507	4421 ± 4
22	$X(4630)$		$5S$	4614	-	4837	4634^{+8+5}_{-7-8}
21	$X(4660)$		$4D$	4641	-	4857	$4664 \pm 11 \pm 5$
17	$\chi_{c1}(1P)$	1^{++}	$1P$	3504	3510	3511	3510.66 ± 0.07
			$2P$	3947	3950	3906	-
			$3P$	4272	-	4319	-
	$\eta_{c2}(1D)$	2^{-+}	$1D$	3812	3840	3807	-
			$2D$	4166	4210	4196	-
			$3D$	4437	-	4549	-
17	$\chi_{c2}(1P)$	2^{++}	$1P$	3532	3550	3555	3556.20 ± 0.09
23	$Z(3930)$		$2P$	3969	3980	3949	$3929 \pm 5 \pm 2$
			$1F$	4043	4010	4041	-
24	$X(3823)$	2^{--}	$1D$	3810	3840	3795	$3823.1 \pm 1.8 \pm 0.7$
			$2D$	4164	4210	4190	-
			$3D$	4436	-	4544	-

3.2. Charmed and charmed-strange mesons

A simple analysis about the properties of hadrons containing a single heavy quark $Q = c, b$ can be carried out in the $m_Q \rightarrow \infty$ limit. In such a limit, the heavy quark acts as a static color source for the rest of the hadron, its spin \vec{s}_Q is decoupled from the total angular momentum of the light degrees of freedom $\vec{j}_q = \vec{s}_q + \vec{l}$, and they are separately conserved. Heavy mesons can be organized in doublets, each one corresponding to a particular value of j_q and parity. The lowest lying $Q\bar{q}$ mesons correspond to $l = 0$ (S -wave states of the quark model) with $j_q^P = \frac{1}{2}^-$. This doublet comprises two states with spin-parity $J^P = (0^-, 1^-)$. For $l = 1$ (P -wave states of the quark model), it could be either $j_q^P = \frac{1}{2}^+$ or $j_q^P = \frac{3}{2}^+$, the two corresponding doublets having $J^P = (0^+, 1^+)$ and $J^P = (1^+, 2^+)$.

However the experimental results show intriguing aspects which contradict this analysis, specially in the charm strange sector. The abnormally light mass of the mesons $D_{s0}^*(2317)$ and $D_{s1}(2460)$ below the DK and D^*K thresholds respectively make these states very narrow since the only allowed decays violate isospin. The unexpected feature of these mesons is that they have masses close (or even lower) than their charmed partners. Moreover the masses predicted by most of the theoretical approaches are considerably heavier than the experimental ones

Very recently new D and D_s resonances has been discovered. Thus BaBar collaboration³² reported four new resonances: $D(2550)^0$, $D(2600)^0$, $D(2750)^0$ and $D^*(2760)^0$. These resonances has been recently confirmed by LHCb collaboration³³ adding two more states $D(3000)^0$ and $D^*(3000)^+$. The results of both collaboration are compatibles except in the case of the width of the $D(2600)^0$ measured as $\Gamma = 93 \pm 6 \pm 13$ by BaBar collaboration and $\Gamma = 140 \pm 17 \pm 18$ by LHCb. Concerning the charmed strange sector three new states has been reported:³⁴ $D_{s1}^*(2710)^+$, $D_{sJ}^*(2860)^+$ and $D_{sJ}^*(3040)^+$. These states has been also confirmed by LHCb collaboration.³⁵

The spectra of D and D_s are given in Table 3 and Table 4. We compare our results with those predicted by other significant quark models in the literature: D. Ebert, R.N. Faustov and V.O. Galkin³⁶ and Di Pierro and Eichten.³⁷ Assignments for the well established states taken from Particle Data Group (PDG)¹⁷ are also given.

The masses predicted for the 0^- and 1^- states – the $j_q^P = \frac{1}{2}^-$ doublet – agree with the experimental measurements in both sectors. The doublet $j_q^P = \frac{3}{2}^+$, which corresponds to the 2^+ state and one of the low lying 1^+ states, is in reasonable agreement with experiment.

As one can see, most of the models cannot reproduce the mass splittings between the $D_{s0}^*(2317)$, $D_{s1}(2460)$ and $D_{s1}(2536)$ mesons. This feature is shared by other quark models, but also by other approaches like lattice QCD calculations.³⁸ The charmed and charmed-strange 0^+ states are sensitive to the one-loop corrections of the OGE potential included in our model which bring their masses closer to experiment. This is in agreement with the conclusion of Ref. 39. However, their

Table 3. Masses, in MeV, of charmed mesons predicted by the constituent quark model. We compare our results with those of other significant quark models in the literature from Refs. 36 and 37. The experimental data are from the PDG.¹⁷

Assignment	J^P	The.	Ref. 36	Ref. 37	Exp.
D	0^-	1896	1871	1868	1867.7 ± 0.3
$D(2550)$		2695	2581	2589	$2539.4 \pm 4.5 \pm 6.8$
		3154	3062	3141	
D^*	1^-	2014	2010	2005	2010.25 ± 0.14
		2754	2632	2692	
		2905	3096	3226	
$D_0(2400)$	0^+	2362	2406	2377	2318 ± 29
		2925	2919	2949	
		3292			
$D_1(2420)$	1^+	2499	2426	2417	2421.4 ± 0.6
$D_1(2430)$		2535	2469	2426	$2427 \pm 26 \pm 25$
		3033	2932	2995	
$D_2(2460)$	2^+	2544	2460	2460	2462.6 ± 0.6
		3059	3012	3035	
	2^-	2822	2806	2775	
		2962	2850	2873	
	3^+	3094	2863	2799	
		3240	3335		
	3^-	2863	3129	3123	
		3260	3145		

contribution are not enough to solve the puzzle in the 1^+ sector. The importance of the meson-meson continuum in the 1^+ $c\bar{s}$ sector will be studied later.

Table 4. Masses, in MeV, of charmed-strange mesons predicted by the constituent quark model. We compare our results with those of other significant quark models in the literature from Refs. 36 and PhysRevD.64.114004 (2001). The experimental data are from the PDG.¹⁷

Assignment	J^P	The.	Ref. 36	Ref. 37	Exp.
D_s	0^-	1984 2729 3178	1969 2688	1965 2750 3259	1968.5 ± 0.32
D_s^*	1^-	2104	2111	2113	2112.3 ± 0.5
$D_{s1}^*(2700)$		2794 2890	2731 2913	2806 2913	2709.0 ± 0.4
$D_{s0}^*(2317)$	0^+	2383 2934 3310	2509	2487 3067	2317.8 ± 0.6
$D_{s1}(2460)$	1^+	2560	2536	2535	2459.6 ± 0.6
$D_{s1}(2526)$		2570 3061	2574	2605 3114	2535.12 ± 0.13
$D_{s2}(2573)$	2^+	2609 3094	2571 3142	2581 3157	2571.9 ± 0.8
	2^-	2888 2943	2931 2961	2900 2953	
	3^+	3151 3215	3254 3266	3203 3247	
	3^-	2922 3304	2971 3469	2925	

We postpone the assignment of the new states to the strong decay section were the strong width of these meson will be present in detail

3.3. Electromagnetic decays

The knowledge of the leptonic decay width of higher 1^{--} charmonium states is important for several reasons. First of all it allows to test the wave function at very short distances. Moreover it can help to distinguish between conventional $c\bar{c}$ mesons and multiquark structures which have much smaller dielectron widths.⁴⁰ The leptonic widths are compared in Table 5, we include the recent data reported by the BES Collaboration in Ref. 41.

As we have mentioned, one striking feature of our model is the new assignment of the $\psi(4415)$. Usually this state has been assigned as a $4S$ state. Our particular choice of the potential includes the new $X(4360)$ as a $4S$ state between the well established $\psi(4160)$ and $\psi(4415)$ which are both predicted as D -wave states. Whether or not

Table 5. Leptonic decay widths, in keV, of ψ states.

(nL)	State	$M_{\text{The.}}$ (MeV)	$\Gamma_{\text{The.}}$ (keV)	$\Gamma_{\text{Exp.}}$ (keV)	
(1S)	J/ψ	3096	3.93	$5.55 \pm 0.14 \pm 0.02$	¹⁷
(2S)	$\psi(2S)$	3703	1.78	2.33 ± 0.07	¹⁷
(1D)	$\psi(3770)$	3796	0.22	0.22 ± 0.05	⁴¹
(3S)	$\psi(4040)$	4097	1.11	0.83 ± 0.20	⁴¹
(2D)	$\psi(4160)$	4153	0.30	0.48 ± 0.22	⁴¹
(4S)	$X(4360)$	4389	0.78	-	-
(3D)	$\psi(4415)$	4426	0.33	0.35 ± 0.12	⁴¹
(5S)	$X(4630)$	4614	0.57	-	-
(4D)	$X(4660)$	4641	0.31	-	-

Table 6. Branching fraction for the decay $\psi(2S) \rightarrow \gamma(\gamma J/\psi)_{\chi_{cJ}}$. Experimental data are from Ref. 43.

Mode	$\Gamma_{\text{The.}}$	$\Gamma_{\text{Exp.}}$
$\gamma(\gamma J/\psi)_{\chi_{c0}}$	0.156	$0.125 \pm 0.007 \pm 0.013$
$\gamma(\gamma J/\psi)_{\chi_{c1}}$	4.423	$3.56 \pm 0.03 \pm 0.12$
$\gamma(\gamma J/\psi)_{\chi_{c2}}$	2.099	$1.95 \pm 0.02 \pm 0.07$

this assignment is correct can be tested with the e^+e^- leptonic widths. From Table 5 one can see that the width of the 4S state is 0.78 keV, whereas the experimental value for the $\psi(4415)$ is $\Gamma_{e^+e^-} = 0.35 \pm 0.12$ keV, in excellent agreement with the result for the 3D state (0.33 keV). The measurement of the leptonic width for the $X(4360)$ is very important and would clarify the situation.

It is generally assumed that the $1^{--} c\bar{c}$ mesons are a mixture of 3S_1 and 3D_1 states in order to reproduce the leptonic widths. In our model the mixing is not fitted to the experimental data but driven by the tensor piece of the quark-antiquark interaction. All are almost pure states either 3S_1 or 3D_1 and we can reasonably reproduce the leptonic widths.

The study of higher multipole contributions to the radiative transitions between spin-triplet states involves an alternative way to disentangle the mixing between S - and D -waves in $1^{--} c\bar{c}$ mesons. The radiative decay sequences

$$e^+e^- \rightarrow \psi(2S), \quad \psi(2S) \rightarrow \gamma' \chi_{(c1,c2)}, \quad \chi_{(c1,c2)} \rightarrow \gamma J/\psi, \quad J/\psi \rightarrow e^+e^- \text{ or } \mu^+\mu^-, \quad (12)$$

has been studied experimentally in Ref. 42. The electric dipole amplitudes are dominant but higher multipole contributions are allowed.

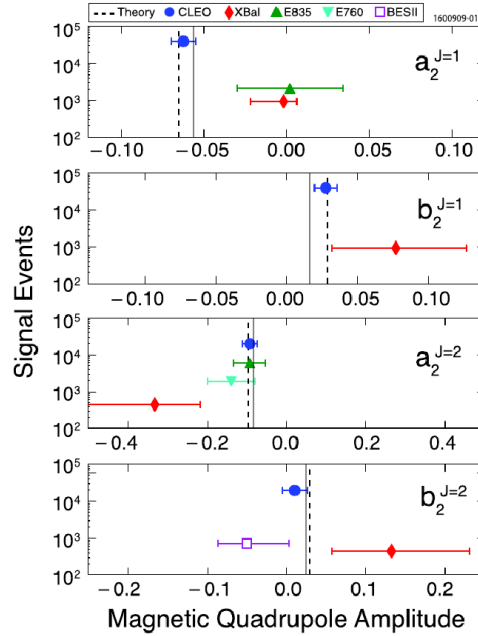


Figure 1. Figure from Ref. 42. Experimental values of the magnetic quadrupole amplitudes obtained by the CLEO Collaboration and their comparison with previous experimental data and theoretical expectations.

For the χ_{cJ} ($J = 1, 2$) sequences, they search for two multipole amplitudes $b_2^{J=1,2}$ and $a_2^{J=1,2}$, where b stands for the amplitude where χ_{cJ} is a reaction product ($\psi' \rightarrow \gamma' \chi_{cJ}$) and a stands for the amplitude where χ_{cJ} is the decay particle ($\chi_{cJ} \rightarrow \gamma J/\psi$).

We show in Fig. 1 the experimental data (solid circles) obtained by the CLEO Collaboration in Ref. 42. The rest of the data are previous to Ref. 42. Our theoretical estimations are represented by a vertical solid line. The same theoretical estimations considering a c -quark mass ($m_c = 1.5$ GeV) closer to the PDG value are represented by a vertical dashed line as given in Ref. 42. The last experimental measurements and the theoretical estimations agree well. In some sense it indicates that the mixing between S and D -waves in the $1^{--} c\bar{c}$ states is small, but also in others as the 2^{++} channel where the mixing is between the P and F -waves.

To end the above discussion, one can calculate the branching fraction of the process $\psi(2S) \rightarrow J/\psi \gamma \gamma$ through $\gamma \chi_{cJ}$. In Table 6 we compare our results with the most recent experimental data.⁴³ We reproduce not only the tendency of the experimental data but also the absolute value.

Table 7 shows the E1 radiative decay widths for the first two states of η_{c2} and ψ_2 that may be useful for experimentalists. The recently reported²⁴ $X(3823)$ state has been assigned to the $1^3D_2 c\bar{c}$ state 2. An upper limit of the branching

Table 7. E1 radiative transitions for the first two states of η_{c2} and ψ_2 .

Initial meson	Final meson	Γ_{CQM} (keV)
$\eta_{c2}(1^1D_2)$	$h_c(1^1P_1)$	276.95
$\eta_{c2}(2^1D_2)$	$h_c(1^1P_1)$	114.66
	$h_c(2^1P_1)$	211.78
$\psi_2(1^3D_2)$	$\chi_{c1}(1^3P_1)$	224.10
	$\chi_{c2}(1^3P_2)$	53.74
$\psi_2(2^3D_2)$	$\chi_{c1}(1^3P_1)$	95.44
	$\chi_{c2}(1^3P_2)$	19.92
	$\chi_{c1}(2^3P_1)$	164.35
	$\chi_{c2}(2^3P_2)$	47.92
	$\chi_{c2}(1^3F_2)$	3.88

ratio $\mathcal{B}(X(3823) \rightarrow \chi_{c2}(1P)\gamma)/\mathcal{B}(\chi_{c1}(1P)\gamma) < 0.41$ has been also given by experimentalists. Our value, 0.24, is below that limit and assures our assignment. The reason why the 1^3D_2 $c\bar{c}$ state has been difficult to observe is that open-flavor decay modes are not allowed. The same situation appears for the 1^1D_2 state being the E1 radiative decays the most plausible decay channels in which this particle can be observed.

4. Strong Decays

Meson strong decay is a complex nonperturbative process that has not yet been described from first principles of QCD. This leads to a rather poorly understood area of hadronic physics which is a problem because decay widths comprise a large portion of our knowledge of the strong interaction.

Several phenomenological models have been developed to deal with this topic. The most popular is the 3P_0 model which assumes that a quark-antiquark pair is created with vacuum quantum numbers, $J^{PC} = 0^{++}$. The 3P_0 model was first proposed by Micu.⁴⁴ Le Yaouanc *et al.* applied subsequently this model to meson⁴⁵ and baryon⁴⁶ open-flavor strong decays in a series of publications in the 1970s.

We calculate in this Section the total decay widths of the mesons which belong to charmed and charmed-strange through a modified version of the 3P_0 model with a scale dependent strength γ of the decay interaction given by .

$$\gamma(\mu) = \frac{\gamma_0}{\log\left(\frac{\mu}{\mu_\gamma}\right)}, \quad (13)$$

where μ is the reduced mass of the $q\bar{q}$ pair of the decaying meson and $\gamma_0 = 0.81 \pm 0.02$

Table 8. Calculated through the 3P_0 model, the strong total decay widths of the mesons which belong to charmed, charmed-strange, hidden charm and hidden bottom sectors. The value of the parameter γ in every quark sector is given by Eq. (13).

Meson	J	P	C	Mass (MeV)	$\Gamma_{\text{Exp.}}$ (MeV) ¹⁷	$\Gamma_{\text{The.}}$ (MeV)
$\psi(3770)$	1	-1	-1	3775.2 ± 1.7	27.6 ± 1.0	26.5 ± 1.7
$\psi(4040)$	1	-1	-1	4039 ± 1	80 ± 10	111.2 ± 7.0
$\psi(4160)$	1	-1	-1	4153 ± 3	103 ± 8	115.9 ± 7.3
$X(4360)$	1	-1	-1	4361 ± 9	74 ± 18	113.9 ± 7.2
$\psi(4415)$	1	-1	-1	4421 ± 4	119 ± 16^{48}	159.0 ± 10.0
$X(4640)$	1	-1	-1	4634 ± 8	92 ± 52	206.3 ± 13.0
$X(4660)$	1	-1	-1	4664 ± 11	48 ± 15	135.0 ± 8.6
$D^*(2010)^\pm$	1	-1	-	2010.25 ± 0.14	0.096 ± 0.022	0.036 ± 0.003
$D_0^*(2400)^\pm$	0	+1	-	2403 ± 38	283 ± 42	212.01 ± 17.1
$D_1(2420)^\pm$	1	+1	-	2423.4 ± 3.1	25 ± 6	25.3 ± 2.0
$D_1(2430)^0$	1	+1	-	2427 ± 36	384 ± 150	229.2 ± 18.5
$D_2^*(2460)^\pm$	2	+1	-	2460.1 ± 4.4	37 ± 6	64.1 ± 5.2
$D(2550)^0$	0	-1	-	2539.4 ± 8.2	130 ± 18	132.1 ± 10.7
$D^*(2600)^0$	1	-1	-	2608.7 ± 3.5	93 ± 14	96.9 ± 7.8
$D_J(2750)^0$	2	-1	-	2752.4 ± 3.2	71 ± 13	229.9 ± 18.6
$D_J^*(2760)^0$	3	-1	-	2763.3 ± 3.3	60.9 ± 6.2	116.4 ± 9.3
$D_{s1}(2536)^\pm$	1	+1	-	2535.12 ± 0.25	1.03 ± 0.13^{49}	0.99 ± 0.07
$D_{s2}^*(2575)^\pm$	2	+1	-	2572.6 ± 0.9	20 ± 5	18.7 ± 1.3
$D_{s1}^*(2710)^\pm$	1	-1	-	2710 ± 14	149 ± 65	170.8 ± 12.1
$D_{sJ}^*(2860)^\pm$	$\begin{bmatrix} 1 \\ 3 \end{bmatrix}$	-1	-	2862 ± 6	48 ± 7	$\begin{bmatrix} 153.2 \pm 10.9 \\ 85.1 \pm 6.1 \end{bmatrix}$
$D_{sJ}(3040)^\pm$	1	+1	-	3044 ± 31	239 ± 71	301.5 ± 21.5

and $\mu_\gamma = 49.84 \pm 2.58$ MeV are parameters determined through the fit to some selected the total decay widths. Reference 47 provides a detailed explanation on how the fit was performed and on the convention for the definition of γ (see Eq. (2) of Ref. 47).

Table 8 shows our results for the total strong decay widths of the mesons which belong to hidden charm, charmed and charmed-strange sectors. In the case of mesons containing a single c -quark, we have considered the newly observed charmed mesons $D(2550)$, $D^*(2600)$, $D_J(2750)$ and $D_J^*(2760)$, and charmed-strange mesons $D_{s1}^*(2710)$, $D_{sJ}^*(2860)$ and $D_{sJ}(3040)$. We get a quite reasonable global description of the total decay widths. A study of the theoretical uncertainties has been performed. It consists on a montecarlo study of the variation of the total decay widths taking into account the uncertainties of the γ parameters in Eq. 13.

The detailed analysis of the decay modes of every resonance is beyond the scope of this report. However, let us comment in more detail each sector discussing briefly

the most significant aspects.

The results predicted by the 3P_0 model for the well established charmed mesons are in good agreement with the experimental data except for one case, the total decay width of the D^* meson. The D^* decays only into $D\pi$ channel via strong interaction and it is assumed that the total decay width is given mainly by this decay mode. However, the disagreement may be due to the very small available phase space which enhances possible effects of the final-state interactions.

With respect to the new states reported by Babar [32], the $J^P = 0^-$ is the most plausible assignment for the $D(2550)$ meson. The total width predicted by the 3P_0 model with this assignment is in very good agreement with the experimental data. The helicity-angle distribution of $D^*(2600)$ is found to be consistent with $J^P = 1^-$. Moreover, its mass makes it the perfect candidate to be the spin partner of the $D(2550)$ meson. The predicted mass is about 100 MeV above the experimental value while our prediction of the total decay width as the 2^3S_1 state agrees with the data Babar data but is in clear disagreement with the LHCb data.

There is a strong discussion in the literature about the possible quantum numbers that could have the mesons $D_J(2750)$ and $D_J^*(2760)$ providing a wide range of assignments. It is important to take into account the experimental observations about these two mesons reported in Ref. [32] before assigning any quantum number. First, despite that the two mesons are close in mass and their total widths are similar, they are considered different particles. Second, the helicity-angle distribution of both mesons is compatible with an angular momentum between quark and antiquark equal to $L = 2$. Third, the $D_J(2750)$ and $D_J^*(2760)$ mesons have only been seen in the decay mode $D^*\pi$ and $D\pi$, respectively. And finally, the following branching ratio has been measured

$$\frac{\mathcal{B}(D_J^*(2760)^0 \rightarrow D^+\pi^-)}{\mathcal{B}(D_J(2750)^0 \rightarrow D^{*+}\pi^-)} = 0.42 \pm 0.05 \pm 0.11. \quad (14)$$

The assignment of the $D_J(2750)$ meson as the $nJ^P = 12^-$ state and the $D_J^*(2760)$ meson as the $nJ^P = 13^-$ state seems the most plausible in our model. This assignment agrees with those of Ref. [50]

The predicted masses are of the order of 100 MeV above the experimental data and we obtain a value of 0.68 for the branching ratio written in Eq. (14). However the predicted widths are in clear disagreement with the experimental ones and the problems with the identification of these two states still remains open.

Our theoretical results are in good agreement with the experimental data in the charmed-strange sector. Two new charmed-strange resonances, $D_{s1}(2710)$ and $D_{sJ}(2860)$, have been observed by the BaBar Collaboration in both DK and D^*K channels.³⁴ In the D^*K channel, the BaBar Collaboration has also found evidence for the $D_{sJ}(3040)$, but there is no signal of $D_{sJ}(3040)$ in the DK channel. It is commonly believed that the $D_{s1}(2710)$ is the first excitation of the D_s^* meson. With this assignment, the prediction of the 3P_0 model is in agreement with the experimental data. In Table 8 we show the total strong decay width of the $D_{sJ}^*(2860)$

as the third excitation of the 1^- meson and as the ground state of the 3^- meson. The comparison between experimental data and our results favors the $n J^P = 1 3^-$ assignment. The $2P$ multiplet mean mass is predicted in our model to be near the mass of the $D_{sJ}(3040)$ resonance. The only decay mode in which the $D_{sJ}(3040)$ has been seen until now is the D^*K , and so the most possible assignment is that the $D_{sJ}(3040)$ meson being the next excitation in the 1^+ channel. Table 8 shows our prediction of the $D_{sJ}(3040)$ decay width as the $n J^P = 3 1^+$ or $4 1^+$ state. Both are large but compatible with the experimental data.

One can see that the general trend of the total decay widths is well reproduced in the $1^{--} c\bar{c}$ sector. There are two particular cases in which the theoretical results exceed the experimental ones. The first case is the $\psi(4415)$ resonance, where we predict a total width of 159 MeV while the PDG average value is 62 ± 20 MeV.¹⁷ However, one should mention that the experimental data are clustered around two values (~ 100 MeV and ~ 50 MeV) corresponding the lower one to very old measurements. If we compare our result with the recent experimental data reported by Seth *et al.*⁴⁸ ($\Gamma = 119 \pm 16$ MeV), they are more compatible. The second result which disagrees with the experimental data is the corresponding to the pair of states in the vicinity of 4.6 GeV. Both widths are larger than the experimental results. The smallest total width of the $X(4660)$ favors the 4^3D_1 option for this state although interference between the two states can be the origin of the disagreement.

4.1. Description of the $D_{s1}(2536)^+$ strong decay properties

Recently, new observables of the $D_{s1}(2536)^+$ have been measured. The BaBar Collaboration has performed a high precision measurement of the $D_{s1}(2536)$ decay width obtaining a value of $(1.03 \pm 0.05 \pm 0.12)$ MeV.⁴⁹ Furthermore, the Belle Collaboration has reported the first observation of the $D_{s1}(2536)^+ \rightarrow D^+\pi^-K^+$ decay measuring the branching fraction⁵¹

$$\frac{D_{s1}(2536)^+ \rightarrow D^+\pi^-K^+}{D_{s1}(2536)^+ \rightarrow D^{*+}K^0} = (3.27 \pm 0.18 \pm 0.37)\%. \quad (15)$$

They also measured the ratio of the S -wave amplitude in the $D_{s1}(2536)^+ \rightarrow D^{*+}K^0$ decay finding a value of $0.72 \pm 0.05 \pm 0.01$.

In order to gain insight into the structure of the 1^+ charmed-strange mesons, we study the reaction $D_{s1}(2536)^+ \rightarrow D^+\pi^-K^+$ as well as the angular decomposition of the $D_{s1}(2536)^+ \rightarrow D^{*+}K^0$ decay.

In the model described in this work, a tetraquark $c\bar{s}n\bar{n}$ state has been predicted by Vijande *et al.* in Ref. 52 with quantum numbers $IJ^P = 01^+$ and mass $M = 2841$ MeV. If this state is present it should be coupled to the $J^P = 1^+$ $c\bar{s}$ states.

Working in the HQS limit, the $c\bar{s}n\bar{n}$ tetraquark has three different spin states, $|0 1/2\rangle$, $|1 1/2\rangle$ and $|1 3/2\rangle$ where the first index denotes the spin of the $n\bar{n}$ pair and the second the coupling with the \bar{s} spin. Although we use the 3P_0 model to calculate

the meson decay widths, a description of the coupling between the D_s meson and the tetraquark based on this model is beyond the scope of the present calculation. However, we use it here to select the dominant couplings and parametrize the vertex as a constant C_S . The model assumes that the $n\bar{n}$ pair created is in a $J = 0$ state which means that the D_s states will only couple with the first tetraquark component which has spin $1/2$ for the three light quarks. In the HQS limit the heavy quark is an spectator and the angular momentum of the light quarks has to be conserved so that the tetraquark will only couple to the $c\bar{s}$ $j_q = 1/2$ state.

For that reason we couple the tetraquark structure with the $j_q = 1/2$ $c\bar{s}$ state. This choice differs from the one performed in Ref. 52 where the tetraquark is only coupled to the 1P_1 state and not to the 3P_1 . However, this choice has several advantages: it has the correct heavy quark limit, it may reproduce the narrow width of the $D_{s1}(2536)^+$ state and it is in agreement with the experimental situation which tells us that the prediction of the heavy quark limit is reasonable for the $j_q = 3/2$ state but not for the $j_q = 1/2$ one.

In this scenario we diagonalize the matrix

$$M = \begin{pmatrix} M_{3P_1} & C_{SO} & \sqrt{\frac{2}{3}} C_S \\ C_{SO} & M_{1P_1} & \sqrt{\frac{1}{3}} C_S \\ \sqrt{\frac{2}{3}} C_S & \sqrt{\frac{1}{3}} C_S & M_{c\bar{s}n\bar{n}} \end{pmatrix}, \quad (16)$$

where $M_{3P_1} = 2571.5$ MeV, $M_{1P_1} = 2576.0$ MeV and $M_{c\bar{s}n\bar{n}} = 2841$ MeV are the masses of the states without couplings, the $C_{SO} = 19.6$ MeV is the coupling induced by the antisymmetric spin-orbit interaction calculated within the model and C_S is the parameter that gives the coupling between the $j_q = 1/2$ component of the 3P_1 and 1P_1 states and the tetraquark. The value of the parameter $C_S = 224$ MeV is fitted to the mass of the $D_{s1}(2460)$. We get the three eigenstates shown in Table 9. There we also show the probabilities of the three components for each state and the relative phases between different components. One can see that the $D_{s1}(2460)$ meson has a sizable non- $q\bar{q}$ component whereas the $D_{s1}(2536)$ is almost a pure $q\bar{q}$ state. The presence of non- $q\bar{q}$ degrees of freedom in the 1^+ $c\bar{s}$ channel enhances the $j_q = 3/2$ component of the $D_{s1}(2536)$ meson. Moreover, a 1^+ state with an important component of $c\bar{s}n\bar{n}$ tetraquark structure is found at 2973 MeV.

We now calculate the different decay widths for the $D_{s1}(2536)^+$ state of Table 9. As expected, the D^*K decay width is narrow $\Gamma = 0.99$ MeV. As the DK decay is suppressed, the total width would be mainly given by the D^*K channel and is in the order of the experimental value $\Gamma_{\text{exp}} = (1.03 \pm 0.05 \pm 0.12)$ MeV measured by BaBar.⁴⁹ Of course the value strongly depends on the 3P_0 γ strength parameter that has been determined before by a global fit of the total decay widths of heavy mesons. It also depends on the fact that we have only coupled the $1/2$ state with the tetraquark making the remaining state a purest $3/2$ which makes it narrower. If we would include an small coupling between the $3/2$ state and the tetraquark our $D_{s1}(2536)$ will be broader.

Table 9. Masses and probability distributions for the three eigenstates obtained from the coupling of the D_s and tetraquark states. The relative sign to the tetraquark component is also shown.

M (MeV)	$S(^3P_1)$	$P(^3P_1)$	$S(^1P_1)$	$P(^1P_1)$	$S(c\bar{s}n\bar{n})$	$P(c\bar{s}n\bar{n})$
2459	—	55.7	—	18.8	+	25.5
2557	+	27.7	—	72.1	+	0.2
2973	+	16.6	+	9.1	+	74.3

Table 10. Width and the three branching ratios defined in the text. The first row shows the experimental data and the second shows our results for the $D_{s1}(2536)$ state given in Table 9. For completeness we give in the last two rows the results for the two 1^+ $c\bar{s}$ states predicted by the naive CQM.

M (MeV)	Γ (MeV)	R_1	R_2	$R_3(\%)$
Exp.	$1.03 \pm 0.05 \pm 0.12$	1.27 ± 0.21	$0.72 \pm 0.05 \pm 0.01$	$3.27 \pm 0.18 \pm 0.37$
2557	0.99	1.31	0.66	14.07
2593	190.17	1.09	1.00	13.13
2554	11.24	1.11	0.97	13.19

There are two other experimental data that do not depend on the γ parameter, namely the branching ratio¹⁷

$$R_1 = \frac{\Gamma(D_{s1}(2536)^+ \rightarrow D^{*0}K^+)}{\Gamma(D_{s1}(2536)^+ \rightarrow D^{*+}K^0)} = 1.27 \pm 0.21, \quad (17)$$

and the ratio of S -wave over the full width for the $D^{*+}K^0$ decay⁵¹

$$R_2 = \frac{\Gamma_S(D_{s1}(2536)^+ \rightarrow D^{*+}K^0)}{\Gamma(D_{s1}(2536)^+ \rightarrow D^{*+}K^0)} = 0.72 \pm 0.05 \pm 0.01. \quad (18)$$

The first branching ratio should be 1 if the isospin symmetry was exact. However, the charge symmetry breaking in the phase space makes it different from this value. The effect is sizable since the $D_{s1}(2536)^+$ is close to the $D^{*+}K$ threshold and for this reason it also depends on the details of the D_{s1} wave function. We get for this ratio the value $R_1 = 1.31$, in good agreement with the experimental one.

Notice that in order to get R_2 different from one, we need to have a state with high $j_q = 3/2$ component. In our case we get a value of $R_2 = 0.66$, close to the experimental data. The fact that our result is smaller than the experimental one indicates that the probability of the $j_q = 3/2$ state is high which is in agreement with the fact that we get a narrower state.

Finally we calculate the branching

$$R_3 = \frac{\Gamma(D_{s1}(2536)^+ \rightarrow D^+\pi^-K^+)}{\Gamma(D_{s1}(2536)^+ \rightarrow D^{*+}K^0)} = (3.27 \pm 0.18 \pm 0.37)\%. \quad (19)$$

As the $D^+\pi^-$ pair in the final state is the only $D\pi$ combination that cannot come from a D^* resonance, we describe the reaction through a virtual D^{*0} meson since $M_{D^{*0}} < M_{D^+} + M_{\pi^-}$. We get $R_3 = 14.1\%$, a factor 3–4 greater than the experimental data. This value seems not to depend on the details of the D_{s1} wave function.

All these results for the width and the ratios R_1 , R_2 and R_3 are summarized in Table 10. We also show, for the sake of completeness, the results for the two 1^+ states without coupling to the $c\bar{s}n\bar{n}$ tetraquark. None of these two states agree with the full set of experimental values.

5. Charmonium resonances in e^+e^- exclusive reactions around the $\psi(4415)$ region

The Belle Collaboration has recently performed measurements of the exclusive cross section for the processes $e^+e^- \rightarrow D^0D^-\pi^+$ ⁵³ and $e^+e^- \rightarrow D^0D^{*-}\pi^+$ ⁵⁴ over the center-of-mass energy range 4.0 GeV to 5.0 GeV. In the first reaction they found a prominent peak in the cross section which is interpreted as the $\psi(4415)$. From the study of the resonant structure in the $\psi(4415)$ decay, they conclude that the final channel $D^0D^-\pi^+$ is reached through the $D\bar{D}_2^*(2460)$ intermediate state. Using a relativistic Breit-Wigner function parametrization, they obtain the value of the $\mathcal{B}(\psi(4415) \rightarrow D\bar{D}_2^*(2460)) \times \mathcal{B}(\bar{D}_2^*(2460) \rightarrow D\pi^+)$ product of branching fractions and the mass and width of the $\psi(4415)$. From the measurement of the $e^+e^- \rightarrow D^0D^{*-}\pi^+$ exclusive cross section reported in Ref. 54, they provide upper limits on the peak cross section for the process $e^+e^- \rightarrow X \rightarrow D^0D^{*-}\pi^+$ where X denotes $X(4260)$, $X(4360)$, $\psi(4415)$, $X(4630)$ and $X(4660)$. Although only the value concerning the $\psi(4415)$ is significant.

We have seen that our assignment of the $\psi(4415)$ as a D -wave state leaving the $4S$ state for the $X(4360)$ agrees with the last measurements of the leptonic and total decay widths. Now we want to perform a study of the two above reactions to test if our result is also compatible with the measurements of Belle.

We assume the reaction $e^+e^- \rightarrow X \rightarrow DD^{(*)}\pi$ and parametrize the cross section using a relativistic Breit-Wigner function including Blatt-Weisskopf corrections. The relativistic Breit-Wigner amplitude for the process “ $e^+e^- \rightarrow \text{resonance} \rightarrow \text{hadronic final state } f$ ” at center-of-mass energy \sqrt{S} can be written as

$$\mathcal{T}_r^f(\sqrt{S}) = \frac{M_r \sqrt{\Gamma_r^{ee}\Gamma_r^f}}{S - M_r^2 + iM_r\Gamma_r} e^{i\delta_r}, \quad (20)$$

where r indicates the resonance being studied, M_r is the nominal mass, Γ_r is the full width, Γ_r^{ee} is the leptonic width, Γ_r^f is the hadronic width for the decaying channel f and δ_r is a relative phase.

When there are more than one resonance in the same energy range and we measure the same decay channel, the spin-averaged cross section is a coherent sum of the Breit-Wigner amplitudes for each resonance

$$\sigma(\sqrt{S}) = \frac{(2J+1)}{(2S_1+1)(2S_2+1)} \frac{16\pi}{S} \left| \sum_r \frac{M_r \sqrt{\Gamma_r^{ee} \Gamma_r^f}}{S - M_r^2 + iM_r \Gamma_r} e^{i\delta_r} \right|^2. \quad (21)$$

Now, we introduce the energy dependence of the widths following Ref. 41. The angular momentum dominant partial width of a resonance decaying into one channel is given by⁵⁵

$$\Gamma_r^f(\sqrt{S}) = \hat{\Gamma}_r \frac{Z_f^{2L+1}}{B_L}, \quad (22)$$

with Z_f defined as $Z_f \equiv \rho P_f$, where P_f is the decay momentum and ρ is a free parameter whose value is around the range of the interaction, in the order of a few fermis. The energy-dependent partial wave functions $B_L(Z_f)$ are given in either Ref. 55 or 56

$$\begin{aligned} B_0 &= 1, \\ B_1 &= 1 + Z_f^2, \\ B_2 &= 9 + 3Z_f^2 + Z_f^4, \\ B_3 &= 225 + 45Z_f^2 + 6Z_f^4 + Z_f^6, \end{aligned} \quad (23)$$

and $\hat{\Gamma}_r$ is related with the partial width at the mass of the resonance, Γ_0 , as

$$\hat{\Gamma}_r = \Gamma_0 \frac{B_L(P_0)}{Z_f^{2L+1}(P_0)}. \quad (24)$$

Then, our final expressions for the partial and total width are given by

$$\begin{aligned} \Gamma_r^f(\sqrt{S}) &= \Gamma_0 \frac{Z_f^{2L+1}(P_f)}{Z_f^{2L+1}(P_0)} \frac{B_L(P_0)}{B_L(P_f)}, \\ \Gamma_r(\sqrt{S}) &= \frac{2M_r}{M_r + \sqrt{S}} \sum_f \Gamma_r^f(\sqrt{S}), \end{aligned} \quad (25)$$

where the term $\frac{2M_r}{M_r + \sqrt{S}}$ is a relativistic correction factor.⁵⁵

5.1. The process $e^+e^- \rightarrow D^0 D^- \pi^+$

This process has been studied by Pakhlova *et al.* in Ref. 53. They perform a separate study of the $e^+e^- \rightarrow D\bar{D}_2^*(2460)$ and $e^+e^- \rightarrow D(D\pi)_{\text{non-}\bar{D}_2^*(2460)}$ concluding that the $e^+e^- \rightarrow D^0 D^- \pi^+$ is dominated by $X \rightarrow D\bar{D}_2^*(2460)$.

Assuming $X \equiv \psi(4415)$ and a relativistic Breit-Wigner function to fit the data, the peak cross section for the process $e^+e^- \rightarrow X \rightarrow D\bar{D}_2^*(2460)$ is $\sigma(e^+e^- \rightarrow \psi(4415)) \times \mathcal{B}(\psi(4415) \rightarrow D\bar{D}_2^*(2460)) \times \mathcal{B}(\bar{D}_2^*(2460) \rightarrow D\pi^+) = (0.74 \pm 0.17 \pm 0.08) \text{ nb}$.

Table 11. Resonance parameters predicted by our constituent quark model for the $X(4360)$ and $\psi(4415)$. The experimental data are taken from Ref. 17 for $X(4360)$ and Ref. 41 for $\psi(4415)$.

	$X(4360)$		$\psi(4415)$	
	Theory	Experiment	Theory	Experiment
Mass (MeV)	4389	$4361 \pm 9 \pm 9$	4426	4415.1 ± 7.9
Γ_{tot} (MeV)	113.9	$74 \pm 15 \pm 10$	159.0	71.5 ± 19.0
Γ_{ee} (keV)	0.78	-	0.33	0.35 ± 0.12

Using

$$\sigma(e^+e^- \rightarrow X) = \frac{12\pi}{m_X^2} \frac{\Gamma_{ee}}{\Gamma_{\text{tot}}}, \quad (26)$$

the authors of Ref. 53 estimate $\mathcal{B}(\psi(4415) \rightarrow D\bar{D}_2^*(2460)) \times \mathcal{B}(\bar{D}_2^*(2460) \rightarrow D\pi^+) = (10.5 \pm 2.4 \pm 3.8)\%$ or $(19.5 \pm 4.5 \pm 9.2)\%$ depending on the different parametrization of the $\psi(4415)$ resonance (Refs. 17 and 41, respectively).

Furthermore, taken from Ref. 17 the branching fraction for $\bar{D}_2^*(2460) \rightarrow D\pi^+$, one can estimate $\mathcal{B}(\psi(4415) \rightarrow DD_2^*) = 0.47$ using the resonance parameters of Ref. 17 or 0.86 using those of Ref. 41. Note that there are two final charged states in the calculation of $\mathcal{B}(\bar{D}_2^*(2460) \rightarrow D\pi^+)$ and we give the branching fraction of the process $\psi(4415) \rightarrow DD_2^*$ in function of the DD_2^* state and not in function of the $D\bar{D}_2^*$ one.

The theoretical calculation of the $e^+e^- \rightarrow D^0D^-\pi^+$ cross section can be divided in three steps. The first one is the resonance production $e^+e^- \rightarrow X$ which can be given in terms of the leptonic width. The second and third steps are the strong decays $\psi(4415) \rightarrow D\bar{D}_2^*(2460)$ and $\bar{D}_2^*(2460) \rightarrow D\pi^+$ which can be calculated using the 3P_0 model. These two partial widths are involved in the calculation of the Γ_r^f in Eq. (21) because in the case under study we have $\Gamma_r^f = \Gamma(X \equiv \psi(4415) \rightarrow D\bar{D}_2^*(2460) \rightarrow DD\pi^+)$ which is equal to $\Gamma(X \equiv \psi(4415) \rightarrow D\bar{D}_2^*(2460)) \times \mathcal{B}(\bar{D}_2^*(2460) \rightarrow D\pi^+)$.

We show the prediction of our model for the mass, the total width and the leptonic width of the resonance $\psi(4415)$ in Table 11. First, we calculate the branching fractions

$$\begin{aligned} \mathcal{B}(D_2^{*+} \rightarrow D^0\pi^+) &= 0.43 \text{ (Exp.: } 0.44 \pm 0.09), \\ \mathcal{B}(\bar{D}_2^{*0} \rightarrow D^-\pi^+) &= 0.43 \text{ (Exp.: } 0.47 \pm 0.03), \end{aligned} \quad (27)$$

which agree with the experimental values of Ref. 17. Furthermore the ratios

$$\begin{aligned} R_1 &= \frac{\Gamma(D_2^{*+} \rightarrow D^0\pi^+)}{\Gamma(D_2^{*+} \rightarrow D^{*0}\pi^+)} = 1.81 \text{ (Exp.: } 1.9 \pm 1.1 \pm 0.3), \\ R_2 &= \frac{\Gamma(\bar{D}_2^{*0} \rightarrow D^-\pi^+)}{\Gamma(\bar{D}_2^{*0} \rightarrow D^{*-}\pi^+)} = 1.81 \text{ (Exp.: } 1.56 \pm 0.16), \end{aligned} \quad (28)$$

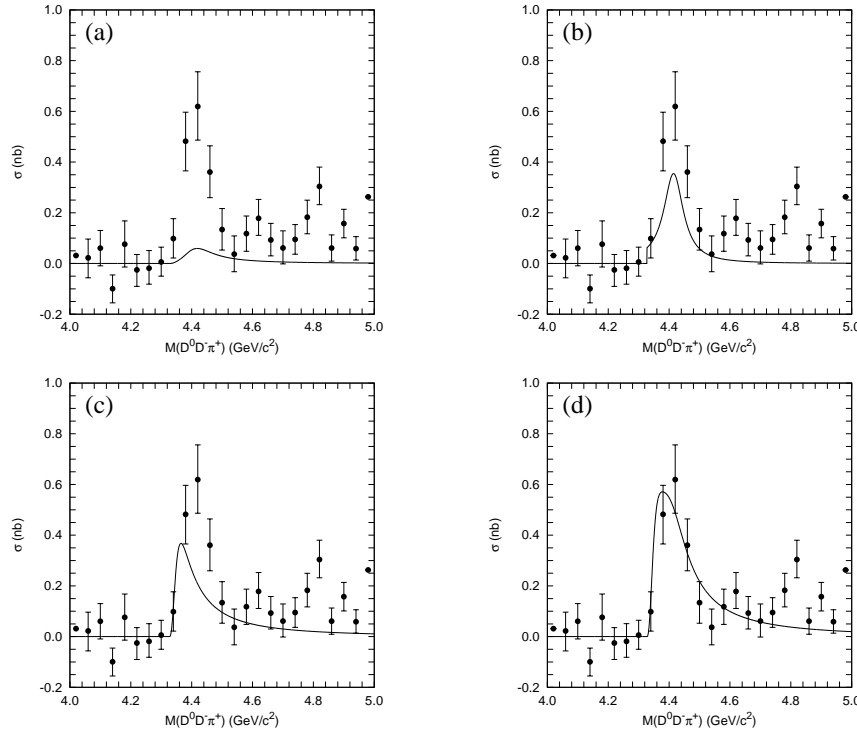


Figure 2. **(a)**: Our model prediction with only the resonance $\psi(4415)$. **(b)**: Model prediction of Ref. 57. **(c)**: Our model prediction with only the resonance $X(4360)$. **(d)**: Our model prediction with the interference of the resonances $X(4360)$ and $\psi(4415)$.

also agree with the experimental data of Ref. 17.

However, when in a similar way we calculate the $\mathcal{B}(\psi(4415) \rightarrow DD_2^*)$, we obtain 0.15 which clearly disagrees with the estimation of Ref. 53.

Our model prediction for the cross section is shown in panel (a) of Fig. 2. One can see that our result is very far from the experimental data. In order to test if this disagreement is due to the $3D$ character of our resonance, we repeat the calculation using the parametrization of Ref. 57 where the $\psi(4415)$ is described as a $4S$ state. Although the result approaches the experimental data, see Fig. 2(b), it still does not describe the full cross section. Certainly, the theoretical results have some uncertainties coming either from the wave functions used in the 3P_0 model or the leptonic width. To minimize these uncertainties we have used in Fig. 2(b) the experimental value for the leptonic width.¹⁷ Using the value $\Gamma_{e^+e^-}$ predicted by the model of Ref. 57, the result would be a factor ~ 3 smaller.

Taken into account that the energy window around the nominal $\psi(4415)$ mass in the experiment of Ref. 53 is ± 100 MeV, we introduce in the calculation the resonance $X(4360)$ which appears as a $4S$ 1^{--} $c\bar{c}$ meson in our model. The predicted

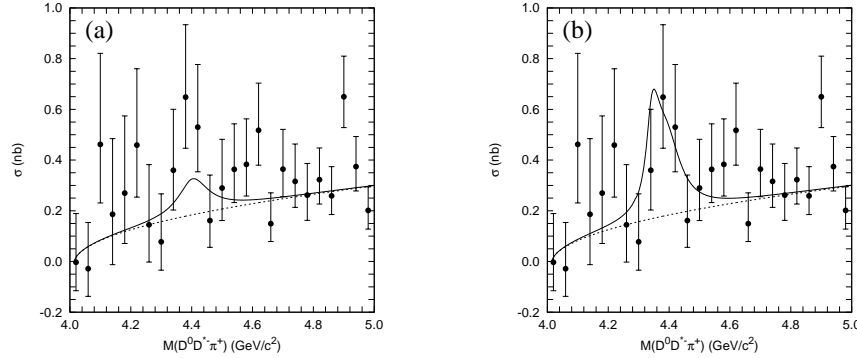


Figure 3. **(a)**: Our model prediction with only the resonance $\psi(4415)$. **(b)**: Our model prediction with the interference of the resonances $X(4360)$ and $\psi(4415)$.

mass, total and leptonic widths are shown in Table 11. Panel (c) of Fig. 2 shows how this resonance alone cannot reproduce the data but the interference between the $X(4360)$ and $\psi(4415)$, panel (d) of Fig. 2, produces a remarkable agreement with the data.

Using the interference of the two resonances, the theoretical value for the exclusive cross section $\sigma(e^+e^- \rightarrow D\bar{D}_2^*(2460) \rightarrow D^0D^-\pi^+)$ at the $\psi(4415)$ mass is 0.48 nb , within the error bars of the experimental one: $(0.62^{+0.14}_{-0.13}) \text{ nb}$. Our result indicates that the two resonances are needed to explain the experimental data.

5.2. The process $e^+e^- \rightarrow D^0D^{*-}\pi^+$

Using the same philosophy we check the $e^+e^- \rightarrow D^0D^{*-}\pi^+$ exclusive cross section measured by the Belle Collaboration.⁵⁴ The experimental analysis estimates from the amplitude of a relativistic Breit-Wigner function fitted to the data an upper limit of 0.76 nb for the peak cross section at $E_{\text{cm}} = M_{\psi(4415)}$.

We calculate the cross section following the same procedure as before. Again the resonance production $e^+e^- \rightarrow X$ has been calculated and is given in Table 11. Now, the second and third steps are the strong decays $\psi(4415) \rightarrow D^{*-}D^{*+}$ and $D^{*+} \rightarrow D^0\pi^+$.

The theoretical result for the branching fraction $\mathcal{B}(D^{*+} \rightarrow D^0\pi^+)$ is 0.687 , in very good agreement with the experimental value 0.677 ± 0.006 of Ref. 17. For the other branching fraction, $\mathcal{B}(\psi(4415) \rightarrow D^*D^*)$, there is no experimental data. Our theoretical result is 0.20 .

The calculation of the cross section including the $\psi(3D)$ resonance with $M = 4426 \text{ MeV}$ alone does not reproduce the full strength of the resonance at $E_{\text{cm}} = M_{\psi(4415)}$ and the result is improved when the $X(4360)$ is added. See Fig. 3.

From the cross section of Fig. 3(b), we calculate the peak cross section for the $e^+e^- \rightarrow D^0D^{*-}\pi^+$ process at $M(D^0D^{*-}\pi^+) = 4415 \text{ MeV}$ obtaining 0.45 nb , which

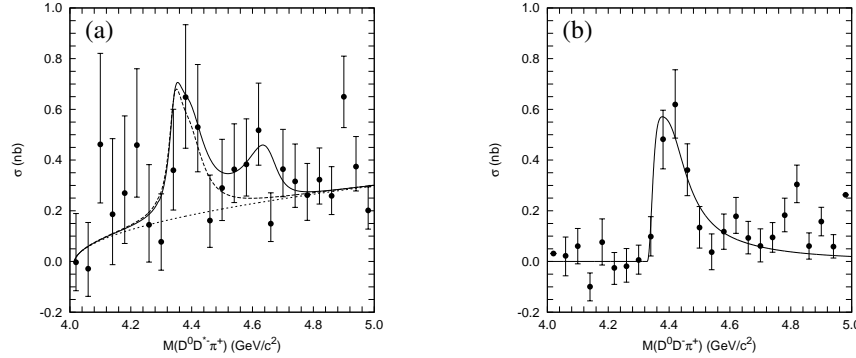


Figure 4. **(a)**: Model prediction of the reaction $e^+e^- \rightarrow D^0 D^{*-} \pi^+$ with the resonances $X(4360)$ and $\psi(4415)$ (dashed line) and including $\psi(5S)$ and $\psi(4D)$ (solid line). **(b)**: Model prediction of the reaction $e^+e^- \rightarrow D^0 D^- \pi^+$ with the resonances $X(4360)$ and $\psi(4415)$ (dashed line) and including $\psi(5S)$ and $\psi(4D)$ (solid line).

is compatible with the experimental upper limit 0.76 nb at 90% C.L. This result is also compatible with the upper limits measured in Ref. 54 for the branchings $\mathcal{B}_{ee} \times \mathcal{B}(X \rightarrow D^0 D^{*-} \pi^+)$ where X denotes the $X(4360)$ and $\psi(4415)$. We obtain the value 0.25×10^{-6} for the $X(4360)$ and 0.35×10^{-6} for the $\psi(4415)$. They should be compared with the upper limits $< 0.72 \times 10^{-6}$ and $< 0.99 \times 10^{-6}$, respectively.

The $X(4360)$ resonance has been sometimes assigned as an unconventional charmonium state since it was discovered in the $e^+e^- \rightarrow \pi^+\pi^-\psi(2S)$ decay²¹ and its open-charm decays were assumed to be suppressed. Ref. 54 gives the branching ratio $\mathcal{B}(X \rightarrow D^0 D^{*-} \pi^+)/\mathcal{B}(X \rightarrow \pi^+\pi^-\psi(2S)) < 8$. Since the $X \rightarrow \pi^+\pi^-\psi(2S)$ is an Okubo-Zweig-Iizuka (OZI) suppressed decay the value of this upper limit means that the open-charm $D^{*+}D^{*-}$ decay, where D^{*+} decays into $D^0\pi^+$, should be small. This is actually the case in our model. We get $\Gamma(D^0 D^{*-} \pi^+) = \Gamma(X(4360) \rightarrow D^{*+}D^{*-})\mathcal{B}(D^{*+} \rightarrow D^0\pi^+) = 3.0 \text{ MeV}$ and combined with the experimental information we obtain $\Gamma(X(4360) \rightarrow \psi(2S)\pi^+\pi^-) \gtrsim 375 \text{ keV}$ which is in the same order of magnitude that other similar decays. The decay of the $\psi(2S)$ meson into $J/\psi\pi\pi$ has a width of 147 keV according to PDG.¹⁷

Finally, data of Ref. 54 show a bump around 4.6 GeV although data of Ref. 53 do not show this bump. Our model predicts two states $\psi(5S)$ and $\psi(4D)$ in this energy region. The inclusion of these two resonances improves the agreement with the cross section in the bump region, as we can see in panel (a) of Fig 4. This bump should not clearly appear in the $e^+e^- \rightarrow D^0 D^- \pi^+$, as one can see in panel (b) of Fig. 4, due to the negligible decay width, predicted by the 3P_0 model, of the $\psi(5S)$ and $\psi(4D)$ states into $DD_2^*(2460)$ channel.

6. Weak Decays

B -factories have become an important source of data on heavy hadrons. Bottomonium states decay mainly into $B\bar{B}$ pairs, and these B mesons decay subsequently into charmed and charmless hadrons via the weak interaction.

To describe theoretically the properties of the mentioned c -quark mesons (conventional or unexpected), one must deal with weak interaction observables which are generally concerned with the semileptonic and nonleptonic decays of b -hadrons. We perform in this Section a study of the semileptonic and nonleptonic B decays into orbitally excited charmed and charmed-strange mesons in order to gain insight on the structure of the charmed mesons.

6.1. Semileptonic B (B_s) decays into D^{**} (D_s^{**}) mesons

Different Collaborations have recently reported semileptonic B decays into orbitally excited charmed mesons providing detailed results of branching fractions. The theoretical analysis of these data, which include both weak and strong decays, offers the possibility for a stringent test of meson models.

The Belle Collaboration reported data⁵⁸ on the product of branching fractions $\mathcal{B}(B^+ \rightarrow D^{**}l^+\nu_l) \mathcal{B}(D^{**} \rightarrow D^{(*)}\pi)$, where, in the usual notation, l stands for a light e or μ lepton. The $D_0^*(2400)$, $D_1(2430)$, $D_1(2420)$ and $D_2^*(2460)$ mesons are denoted generically as D^{**} , and the D^* and D mesons as $D^{(*)}$.

D^{**} decays are reconstructed in the decay chains $D^{**} \rightarrow D^*\pi^\pm$ and $D^{**} \rightarrow D\pi^\pm$. In particular, the $D_0^*(2400)$ meson decays only through the $D\pi$ channel, while the $D_1(2430)$ and $D_1(2420)$ mesons decay only via $D^*\pi$. Both $D\pi$ and $D^*\pi$ channels are opened for $D_2^*(2460)$.

In the case of BaBar data^{59,60} the branching fractions $\mathcal{B}(D_2^*(2460) \rightarrow D^{(*)}\pi)$ include both the D^* and D contributions. As they also provide the ratio $\mathcal{B}_{D/D^{(*)}}$, we estimate separately the D^* and D contributions.

A similar analysis can be done in the charmed strange sector for the B_s meson semileptonic decays. Here the intermediate states are the orbitally charmed-strange mesons, D_s^{**} , and the available final channels are DK and D^*K . The PDG only reports the value of the following product of branching fractions $\mathcal{B}(B_s^0 \rightarrow D_{s1}(2536)^-\mu^+\nu_\mu)\mathcal{B}(D_{s1}(2536)^- \rightarrow D^{*-}\bar{K}^0) = 2.4 \pm 0.7^{17}$ based on their best value for $\mathcal{B}(\bar{b} \rightarrow B_s^0)$ and the experimental data for $\mathcal{B}(\bar{b} \rightarrow B_s^0)\mathcal{B}(B_s^0 \rightarrow D_{s1}(2536)^-\mu^+\nu_\mu)\mathcal{B}(D_{s1}(2536)^- \rightarrow D^{*-}\bar{K}^0)$ measured by the D0 Collaboration.⁶¹

All these magnitudes can be consistently calculated in the framework of constituent quark models because they can simultaneously account for the hadronic part of the weak process and the strong meson decays. In this context, meson strong decays will be described through the 3P_0 model presented before. As for the weak process the matrix elements factorize into a leptonic and a hadronic part. It is the hadronic part that contains the nonperturbative strong interaction effects and we will evaluate it within our constituent quark model. Further details on the semileptonic decay calculation can be found on Refs. 62, 63, 64.

Table 12. Probability distributions and their relative phases for the four states predicted by CQM. In the 1^+ strange sector the effects of non- $q\bar{q}$ components are included; see text for details.

	$D_0^*(2400)$	$D_1(2420)$	$D_1(2430)$	$D_2^*(2460)$
3P_0	+, 1.0000	-	-	-
1P_1	-	-, 0.5903	-, 0.4097	-
3P_1	-	+, 0.4097	-, 0.5903	-
3P_2	-	-	-	+, 0.99993
$1/2, 0^+$	+, 1.0000	-	-	-
$1/2, 1^+$	-	+, 0.0063	-, 0.9937	-
$3/2, 1^+$	-	+, 0.9937	+, 0.0063	-
$3/2, 2^+$	-	-	-	+, 0.99993
	$D_{s0}^*(2317)$	$D_{s1}(2536)$	$D_{s1}(2460)$	$D_{s2}^*(2573)$
3P_0	+, 1.0000	-	-	-
1P_1	-	-, 0.7210	-, 0.1880	-
3P_1	-	+, 0.2770	-, 0.5570	-
3P_2	-	-	-	+, 0.99991
$1/2, 0^+$	+, 1.0000	-	-	-
$1/2, 1^+$	-	-, 0.0038	-, 0.7390	-
$3/2, 1^+$	-	+, 0.9942	-, 0.0060	-
$3/2, 2^+$	-	-	-	+, 0.99991

The mesons involved in the reactions have been discussed in previous sections of this work. The most relevant features to take into account here are: we have reached a good description of the singlet- and triplet-spin S -wave charmed mesons, D and D^* , and charmed-strange mesons, D_s and D_s^* . We have seen that the interpretation of the $D_{s0}^*(2317)$ as a canonical $c\bar{s}$ state is plausible since its mass goes down to the experimental value when the one-loop QCD corrections to the OGE potential are taken into account. The $D_{s1}(2460)$ meson has an important non- $q\bar{q}$ contribution. The presence of non- $q\bar{q}$ degrees of freedom in the $J^P = 1^+$ charmed-strange meson sector enhances the $j_q = 3/2$ component of the $D_{s1}(2536)$ meson, which is almost a pure $q\bar{q}$ state. Table 12 shows only the $q\bar{q}$ probabilities of the orbitally excited charmed and charmed strange mesons.

Table 13 shows the final results and their comparison with the experimental data in the case of the B semileptonic decays into orbitally excited charmed mesons.

The meson $D_0^*(2400)$ has $J^P = 0^+$ quantum numbers and, therefore, due to parity conservation, it decays only into $D\pi$, so that we have $\mathcal{B}(\bar{D}_0^*(2400)^0 \rightarrow$

Table 13. Most recent experimental measurements reported by the Belle and BaBar Collaborations and their comparison with our results. l stands for a light e or μ lepton. The symbol (*) indicates the estimated results from the original data using $B_{D/D(*)}$.

	Belle ⁵⁸ ($\times 10^{-3}$)	BaBar ^{59,60} ($\times 10^{-3}$)	Theory ($\times 10^{-3}$)
$D_0^*(2400)$			
$\mathcal{B}(B^+ \rightarrow \bar{D}_0^*(2400)^0 l^+ \nu_l) \mathcal{B}(\bar{D}_0^*(2400)^0 \rightarrow D^- \pi^+)$	$2.4 \pm 0.4 \pm 0.6$	$2.6 \pm 0.5 \pm 0.4$	2.15
$\mathcal{B}(B^0 \rightarrow D_0^*(2400)^- l^+ \nu_l) \mathcal{B}(D_0^*(2400)^- \rightarrow \bar{D}^0 \pi^-)$	$2.0 \pm 0.7 \pm 0.5$	$4.4 \pm 0.8 \pm 0.6$	1.80
$D_1(2430)$			
$\mathcal{B}(B^+ \rightarrow \bar{D}_1(2430)^0 l^+ \nu_l) \mathcal{B}(\bar{D}_1(2430)^0 \rightarrow D^{*-} \pi^+)$	< 0.7	$2.7 \pm 0.4 \pm 0.5$	1.32
$\mathcal{B}(B^0 \rightarrow D_1(2430)^- l^+ \nu_l) \mathcal{B}(D_1(2430)^- \rightarrow \bar{D}^{*0} \pi^-)$	< 5	$3.1 \pm 0.7 \pm 0.5$	1.23
$D_1(2420)$			
$\mathcal{B}(B^+ \rightarrow \bar{D}_1(2420)^0 l^+ \nu_l) \mathcal{B}(\bar{D}_1(2420)^0 \rightarrow D^{*-} \pi^+)$	$4.2 \pm 0.7 \pm 0.7$	$2.97 \pm 0.17 \pm 0.17$	2.57
$\mathcal{B}(B^0 \rightarrow D_1(2420)^- l^+ \nu_l) \mathcal{B}(D_1(2420)^- \rightarrow \bar{D}^{*0} \pi^-)$	$5.4 \pm 1.9 \pm 0.9$	$2.78 \pm 0.24 \pm 0.25$	2.39
$D_2^*(2460)$			
$\mathcal{B}(B^+ \rightarrow \bar{D}_2^*(2460)^0 l^+ \nu_l) \mathcal{B}(\bar{D}_2^*(2460)^0 \rightarrow D^- \pi^+)$	$2.2 \pm 0.3 \pm 0.4$	$1.4 \pm 0.2 \pm 0.2^{(*)}$	1.43
$\mathcal{B}(B^+ \rightarrow \bar{D}_2^*(2460)^0 l^+ \nu_l) \mathcal{B}(\bar{D}_2^*(2460)^0 \rightarrow D^{*-} \pi^+)$	$1.8 \pm 0.6 \pm 0.3$	$0.9 \pm 0.2 \pm 0.2^{(*)}$	0.79
$\mathcal{B}(B^+ \rightarrow \bar{D}_2^*(2460)^0 l^+ \nu_l) \mathcal{B}(\bar{D}_2^*(2460)^0 \rightarrow D^{(*)-} \pi^+)$	$4.0 \pm 0.7 \pm 0.5$	$2.3 \pm 0.2 \pm 0.2$	2.22
$\mathcal{B}(B^0 \rightarrow D_2^*(2460)^- l^+ \nu_l) \mathcal{B}(D_2^*(2460)^- \rightarrow \bar{D}^0 \pi^-)$	$2.2 \pm 0.4 \pm 0.4$	$1.1 \pm 0.2 \pm 0.1^{(*)}$	1.34
$\mathcal{B}(B^0 \rightarrow D_2^*(2460)^- l^+ \nu_l) \mathcal{B}(D_2^*(2460)^- \rightarrow \bar{D}^{*0} \pi^-)$	< 3	$0.7 \pm 0.2 \pm 0.1^{(*)}$	0.74
$\mathcal{B}(B^0 \rightarrow D_2^*(2460)^- l^+ \nu_l) \mathcal{B}(D_2^*(2460)^- \rightarrow \bar{D}^{(*)0} \pi^-)$	< 5.2	$1.8 \pm 0.3 \pm 0.1$	2.08
$B_{D/D^{(*)}}$	0.55 ± 0.03	$0.62 \pm 0.03 \pm 0.02$	0.65

$D^- \pi^+ = \mathcal{B}(D_0^*(2400)^- \rightarrow \bar{D}^0 \pi^-) = 2/3$ coming from isospin symmetry. One can see in Table 13 that the theoretical product of branching fractions agrees well with the latest BaBar data. The difference between the semileptonic width of the charged and neutral B mesons is due to the large mass difference between the $D_0^*(2400)^0$ and $D_0^*(2400)^\pm$ mesons for which we take the masses reported in Ref. 17.

The only OZI-allowed decay channel for the $D_1(2430)$ meson is the $D_1(2430) \rightarrow D^* \pi$ so that isospin symmetry predicts a branching fraction $\mathcal{B}(D_1(2430) \rightarrow D^* \pi^\pm) = 2/3$. We have in this case for the product of branching fractions shown in Table 13 that our value is roughly a factor of 2 smaller than the results from the BaBar Collaboration.⁵⁹ Note however the disagreement between BaBar and Belle data for the product of branching fractions in which the $\bar{D}_1(2430)^0$ meson is involved.

As in the previous case, the branching fraction $\mathcal{B}(D_1(2420) \rightarrow D^* \pi^\pm)$ is again $2/3$ in our model because $D_1(2420) \rightarrow D^* \pi$ is the only OZI-allowed decay channel. The products of branching fractions compare very well with the latest BaBar data,⁶⁰

Table 14. Open-flavor strong branching ratios for $D_2^*(2460)$ meson calculated through the 3P_0 model and their comparison with those collected by the PDG.¹⁷

Branching ratio	Theory	Experiment
$\Gamma(D_2^{*+} \rightarrow D^0\pi^+)/\Gamma(D_2^{*+} \rightarrow D^{*0}\pi^+)$	1.80	$1.9 \pm 1.1 \pm 0.3$
$\Gamma(D_2^{*0} \rightarrow D^+\pi^-)/\Gamma(D_2^{*0} \rightarrow D^{*+}\pi^-)$	1.82	1.56 ± 0.16
$\Gamma(D_2^* \rightarrow D\pi)/\Gamma(D_2^* \rightarrow D^{(*)}\pi)$	0.65	$0.62 \pm 0.03 \pm 0.02$

as seen in Table 13.

The strong decays which appear in the decay chains that involve the $D_2^*(2460)$ meson are $D_2^*(2460) \rightarrow D\pi^-$ and $D_2^*(2460) \rightarrow D^*\pi^-$. In Table 14 we show the strong decay branching ratios obtained with the 3P_0 model. They are in good agreement with experimental data.¹⁷ Considering that the total width of the $D_2^*(2460)$ meson is the sum of the partial widths of $D\pi$ and $D^*\pi$ channels, since these are the only OZI-allowed processes, we are able to predict the products of branching fractions in Table 13 which are in very good agreement with BaBar data.⁶⁰

The semileptonic decays of B_s meson into orbitally excited charmed-strange mesons (D_s^{**}) provides an extra opportunity to get more insight into the structure of these latter mesons.

We have calculated the semileptonic B_s decays assuming that the D_s^{**} mesons are pure $q\bar{q}$ systems. For the $D_{s0}^*(2317)$ and $D_{s1}(2460)$, which are below the corresponding DK and D^*K thresholds, we only quote the weak decay branching fractions. Concerning the $D_{s1}(2460)$, the 1P_1 and 3P_1 probabilities change with the coupling to non- $q\bar{q}$ degrees of freedom. What we do here is to vary these probabilities (including the phase) in order to obtain the limits of the decay width in the case of the $D_{s1}(2460)$ being a pure $q\bar{q}$ state, see Fig. 5. Assuming that non- $q\bar{q}$ components will give a small contribution to the weak decay, experimental results lower than these limits will be an indication of a more complex structure for this meson.

For the decay into $D_{s1}(2536)$, our model predicts the weak decay branching fraction $\mathcal{B}(B_s^0 \rightarrow D_{s1}(2536)\mu^+\nu_\mu) = 4.77 \times 10^{-3}$ and the strong branching fraction $\mathcal{B}(D_{s1}(2536)^- \rightarrow D^{*-}\bar{K}^0) = 0.43$. The final result appears in Table 15. It is compatible with the existing experimental data,¹⁷ which to us is a confirmation of our result about the $q\bar{q}$ nature of this state.

In the case of the $D_{s2}^*(2573)$ meson the open strong decays are DK and D^*K , so the experimental measurements must be referred to $\mathcal{B}(B_s^0 \rightarrow D_{s2}^*(2573)^-\mu^+\nu_\mu)$, $\mathcal{B}(D_{s2}^*(2573)^- \rightarrow D^-\bar{K}^0)$ and $\mathcal{B}(B_s^0 \rightarrow D_{s2}^*(2573)^-\mu^+\nu_\mu)\mathcal{B}(D_{s2}^*(2573)^- \rightarrow D^{*-}\bar{K}^0)$. For the weak branching fraction we get in this case $\mathcal{B}(B_s^0 \rightarrow D_{s2}^*(2573)^-\mu^+\nu_\mu) = 3.76 \times 10^{-3}$. For the strong decay part of the reaction, we

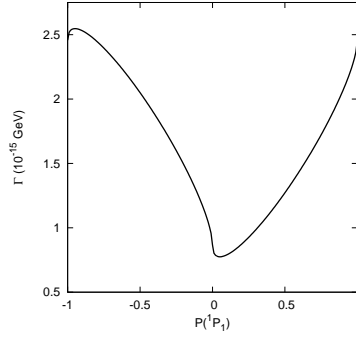


Figure 5. Decay width for the $B_s^0 \rightarrow D_{s1}(2460)^- \mu^+ \nu_\mu$ decay as a function of the 1P_1 component probability. The sign reflects the relative phase between 1P_1 and 3P_1 components: -1 opposite phase and $+1$ same phase.

Table 15. Our predictions and their comparison with the available experimental data for semileptonic B_s decays into orbitally excited charmed-strange mesons.

	Experiment ($\times 10^{-3}$)	Theory ($\times 10^{-3}$)
$D_{s0}^*(2317)$		
$\mathcal{B}(B_s^0 \rightarrow D_{s0}^*(2318)^- \mu^+ \nu_\mu)$	-	4.43
$D_{s1}(2460)$		
$\mathcal{B}(B_s^0 \rightarrow D_{s1}(2460)^- \mu^+ \nu_\mu)$	-	1.74 – 5.70
$D_{s1}(2536)$		
$\mathcal{B}(B_s^0 \rightarrow D_{s1}(2536)^- \mu^+ \nu_\mu) \mathcal{B}(D_{s1}(2536)^- \rightarrow D^{*-} \bar{K}^0)$	$2.4 \pm 0.7^{17,61}$	2.05
$D_{s2}^*(2573)$		
$\mathcal{B}(B_s^0 \rightarrow D_{s2}^*(2573)^- \mu^+ \nu_\mu) \mathcal{B}(D_{s2}^*(2573)^- \rightarrow D^- \bar{K}^0)$	-	1.70
$\mathcal{B}(B_s^0 \rightarrow D_{s2}^*(2573)^- \mu^+ \nu_\mu) \mathcal{B}(D_{s2}^*(2573)^- \rightarrow D^{*-} \bar{K}^0)$	-	0.18
$\mathcal{B}(B_s^0 \rightarrow D_{s2}^*(2573)^- \mu^+ \nu_\mu) \mathcal{B}(D_{s2}^*(2573)^- \rightarrow D^{(*)-} \bar{K}^0)$	-	1.88

obtain

$$\begin{aligned}
 \mathcal{B}(D_{s2}^{*-} \rightarrow D^- \bar{K}^0) &= 0.45 \\
 \mathcal{B}(D_{s2}^{*-} \rightarrow D^{*-} \bar{K}^0) &= 0.047
 \end{aligned}
 \tag{29}$$

using the 3P_0 model. Besides we predict the ratio

$$\frac{\Gamma(D_{s2}^* \rightarrow DK)}{\Gamma(D_{s2}^* \rightarrow DK) + \Gamma(D_{s2}^* \rightarrow D^*K)} = 0.91. \quad (30)$$

Our final results can be seen in Table. 15.

6.2. Nonleptonic B decays into $D^{(*)}D_{sJ}$ final states

The nonleptonic decays of B mesons have been used to search for new charmonium and charmed-strange mesons and to study their properties in detail. For instance, the properties of the $D_{s0}^*(2317)$ and $D_{s1}(2460)$ mesons were not well known until the Belle Collaboration observed the $B \rightarrow \bar{D}D_{s0}^*(2317)$ and $B \rightarrow \bar{D}D_{s1}(2460)$ decays.⁶⁵

First observations of the $B \rightarrow \bar{D}^{(*)}D_{s1}(2536)$ decay modes have been reported by BaBar^{66,67} and an upper limit on the decay $B^0 \rightarrow D^{*-}D_{s1}(2536)^+$ was also obtained by Belle.⁶⁸ The most recent analysis of the production of $D_{s1}(2536)^+$ in double charmed B meson decays has been reported by the Belle Collaboration in Ref. 69. Using the latest measurements of the $B \rightarrow D^{(*)}D_{sJ}$ branching fractions,¹⁷ they calculated the ratios

$$\begin{aligned} R_{D0} &= \frac{\mathcal{B}(B \rightarrow DD_{s0}^*(2317))}{\mathcal{B}(B \rightarrow DD_s)} = 0.10 \pm 0.03, \\ R_{D^*0} &= \frac{\mathcal{B}(B \rightarrow D^*D_{s0}^*(2317))}{\mathcal{B}(B \rightarrow D^*D_s)} = 0.15 \pm 0.06, \\ R_{D1} &= \frac{\mathcal{B}(B \rightarrow DD_{s1}(2460))}{\mathcal{B}(B \rightarrow DD_s^*)} = 0.44 \pm 0.11, \\ R_{D^*1} &= \frac{\mathcal{B}(B \rightarrow D^*D_{s1}(2460))}{\mathcal{B}(B \rightarrow D^*D_s^*)} = 0.58 \pm 0.12. \end{aligned} \quad (31)$$

In addition, the same ratios were calculated for $B \rightarrow D^{(*)}D_{s1}(2536)^+$ decays using combined results by the BaBar⁶⁷ and Belle⁶⁹ Collaborations

$$\begin{aligned} R_{D1'} &= \frac{\mathcal{B}(B \rightarrow DD_{s1}(2536))}{\mathcal{B}(B \rightarrow DD_s^*)} = 0.049 \pm 0.010, \\ R_{D^*1'} &= \frac{\mathcal{B}(B \rightarrow D^*D_{s1}(2536))}{\mathcal{B}(B \rightarrow D^*D_s^*)} = 0.044 \pm 0.010. \end{aligned} \quad (32)$$

From a theoretical point of view, this kind of decays can be described using the factorization approximation.⁶² This amounts to evaluate the matrix element which describes the $B \rightarrow D^{(*)}D_{sJ}$ weak decay process as a product of two matrix elements, the first one to describe the B weak transition into the $D^{(*)}$ meson and the second one for the weak creation of the $c\bar{s}$ pair which makes the D_{sJ} meson. The latter matrix element is proportional to the corresponding D_{sJ} meson decay constant.

The D_{sJ} meson decay constants are not known experimentally except for the ground state, D_s , which has been measured by different Collaborations. Another way to study D_{sJ} mesons, that does not rely on the knowledge of their decay

constants, is through the decays $B_s \rightarrow D_{sJ}M$, where M is a meson with a well known decay constant. However, the experimental study of these processes is currently difficult for several reasons. First, B -factories would need to collect data at the $\Upsilon(5S)$ resonance. Second, the kinematically clean environment of B meson decays does not hold in B_s decays. And finally, the fraction of events with a pair of B_s mesons over the total number of events with a pair of b -flavored hadrons has been measured to be relatively small, $f_s[\Upsilon(5S)] = 0.193 \pm 0.029$. These difficulties leave, for the time being, the $B \rightarrow D^{(*)}D_{sJ}$ decay processes as our best option to study D_{sJ} meson properties.

According to Refs. 70 and 71, within the factorization approximation and in the heavy quark limit, the ratios in Eqs. (31) and (32) can be written as

$$\begin{aligned} R_{D0} &= R_{D^*0} = \left| \frac{f_{D_{s0}^*(2317)}}{f_{D_s}} \right|^2, \\ R_{D1} &= R_{D^*1} = \left| \frac{f_{D_{s1}(2460)}}{f_{D_s^*}} \right|^2, \\ R_{D1'} &= R_{D^*1'} = \left| \frac{f_{D_{s1}(2536)}}{f_{D_s^*}} \right|^2, \end{aligned} \quad (33)$$

where the phase space effects are neglected because they are subleading in the heavy quark expansion. Now, in the heavy quark limit one has $f_{D_{s0}^*(2317)} = f_{D_{s1}(2460)}$, $f_{D_s} = f_{D_s^*}$ and $f_{D_{s1}(2536)} = 0$. Moreover, there are several estimates of the decay constants, always in the heavy quark limit,^{72–74} that predict for P -wave, $j_q = 1/2$ states similar decay constants as for the ground state mesons (i.e. $f_{D_{s0}^*(2317)} = f_{D_s}$ and $f_{D_{s1}(2460)} = f_{D_s^*}$), and very small decay constants for P -wave, $j_q = 3/2$ states. Thus, in the heavy quark limit one would expect $R_{D0} \sim 1$, $R_{D1} \sim 1$ and $R_{D1'} \ll 1$. While the decay into $D_{s1}(2536)$ follows the expectations, this is not the case for the $D_{s0}^*(2317)$ and $D_{s1}(2460)$ mesons. This fact has motivated to argue that either those two states are not canonical $c\bar{s}$ mesons or that the factorization approximation does not hold for decays involving those particles.

Leaving aside that the factorization approximation has been recently analyzed in Refs. 75, 76, 77 finding that it works well in this kind of processes, we will concentrate in the influence of the effect of the finite c -quark mass in the theoretical predictions. As found in Ref. 78, $1/m_Q$ contributions give large corrections to various quantities describing $B \rightarrow D^{**}$ transitions and we expect they also play an important role in this case. It is possible that taking into account the finite mass of the charmed quark one can distinguish better between $q\bar{q}$ and non- $q\bar{q}$ structures for the D_{sJ} mesons.

The nonleptonic decay width for $B \rightarrow D^{(*)}D_{sJ}$ processes in the factorization approximation and using helicity formalism^{62,63} is given in Ref. 79. Using

experimental masses we obtain the ratios

$$\begin{aligned} R_{D0} &= 0.90 \times \left| \frac{f_{D_{s0}^*(2317)}}{f_{D_s}} \right|^2, \\ R_{D^*0} &= 0.72 \times \left| \frac{f_{D_{s0}^*(2317)}}{f_{D_s}} \right|^2. \end{aligned} \quad (34)$$

The double ratio R_{D^*0}/R_{D0} does not depend on decay constants, and in our model we obtain $R_{D^*0}/R_{D0} = 0.80$. The experimental value is given by $R_{D^*0}/R_{D0} = 1.50 \pm 0.75$. Our result is small compared to the central experimental value but we are compatible within 1σ . In the case of the meson $D_{s1}(2460)$ we obtain

$$\begin{aligned} R_{D1} &= 0.70 \times \left| \frac{f_{D_{s1}(2460)}}{f_{D_s^*}} \right|^2, \\ R_{D^*1} &= 1.00 \times \left| \frac{f_{D_{s1}(2460)}}{f_{D_s^*}} \right|^2, \end{aligned} \quad (35)$$

and for the double ratio R_{D^*1}/R_{D1} we get 1.43, which agrees well with the experimental result $R_{D^*1}/R_{D1} = 1.32 \pm 0.43$. Finally, for the meson $D_{s1}(2536)$ we obtain

$$\begin{aligned} R_{D1'} &= 0.64 \times \left| \frac{f_{D_{s1}(2536)}}{f_{D_s^*}} \right|^2, \\ R_{D^*1'} &= 0.99 \times \left| \frac{f_{D_{s1}(2536)}}{f_{D_s^*}} \right|^2, \end{aligned} \quad (36)$$

and for the double ratio $R_{D^*1'}/R_{D1'}$, our value is 1.56 which in this case is 2σ above the experimental one, 0.90 ± 0.27 .

The quality of the experimental numbers does not allow to be very conclusive as to the goodness of the factorization approximation. But one can conclude from Eqs. (34), (35) and (36) that the phase-space and weak matrix element corrections cannot be ignored, as done when using the infinite heavy quark mass limit.

The decay constants of pseudoscalar and vector mesons in charmed and charmed-strange sectors are given in Table 16. We compare our results with the experimental data and those predicted by different approaches and collected in Refs. 17, 80. Our original values are those with the symbol (\dagger). The decay constants of vector mesons agree with other approaches. In the case of the pseudoscalar mesons, the decay constants are simply too large. The reason for that is the following: Our CQM presents an OGE potential which has a spin-spin contact hyperfine interaction that is proportional to a Dirac delta function, conveniently regularized, at the origin. The corresponding regularization parameter was fitted to determine the hyperfine splittings between the n^1S_0 and n^3S_1 states in the different flavor sectors, achieving a good agreement in all of them. While most of the physical observables are insensitive to the regularization of this delta term, those related with annihilation processes are affected. The effect is very small in the 3S_1 channel as

Table 16. Theoretical predictions of decay constants for pseudoscalar and vector charmed mesons. The data have been taken from Ref. 17 for pseudoscalar mesons and from Ref. 80 for vector mesons. PQL \equiv Partially-Quenched Lattice calculation, QL \equiv Quenched Lattice calculations, RBS \equiv Relativistic Bethe-Salpeter, RQM \equiv Relativistic Quark Model, BS \equiv Bethe-Salpeter Method and RM \equiv Relativistic Mock meson model. See the text for the meaning of symbols \dagger and \ddagger .

Approach	f_D (MeV)	f_{D_s} (MeV)	f_{D_s}/f_D
Ours	297.019 ^(†) 214.613 ^(‡)	416.827 ^(†) 286.382 ^(‡)	1.40 ^(†) 1.33 ^(‡)
Experiment	206.7 \pm 8.9	257.5 \pm 6.1	1.25 \pm 0.06
Lattice (HPQCD+UKQCD)	208 \pm 4	241 \pm 3	1.162 \pm 0.009
Lattice (FNAL+MILC+HPQCD)	217 \pm 10	260 \pm 10	1.20 \pm 0.02
PQL	197 \pm 9	244 \pm 8	1.24 \pm 0.03
QL (QCDSF)	206 \pm 6 \pm 3 \pm 22	220 \pm 6 \pm 5 \pm 11	1.07 \pm 0.02 \pm 0.02
QL (Taiwan)	235 \pm 8 \pm 14	266 \pm 10 \pm 18	1.13 \pm 0.03 \pm 0.05
QL (UKQCD)	210 \pm 10 ⁺¹⁷ ₋₁₆	236 \pm 8 ⁺¹⁷ ₋₁₄	1.13 \pm 0.02 ^{+0.04} _{-0.02}
QL	211 \pm 14 ⁺² ₋₁₂	231 \pm 12 ⁺⁶ ₋₁	1.10 \pm 0.02
QCD Sum Rules	177 \pm 21	205 \pm 22	1.16 \pm 0.01 \pm 0.03
QCD Sum Rules	203 \pm 20	235 \pm 24	1.15 \pm 0.04
Field Correlators	210 \pm 10	260 \pm 10	1.24 \pm 0.03
Light Front	206	268.3 \pm 19.1	1.30 \pm 0.04
Approach	f_{D^*} (MeV)	$f_{D_s^*}$ (MeV)	$f_{D_s^*}/f_{D^*}$
Ours	247.865 ^(†)	329.441 ^(†)	1.33 ^(†)
RBS	340 \pm 22	375 \pm 24	1.10 \pm 0.06
RQM	315	335	1.06
QL (Italy)	234	254	1.04 \pm 0.01 ⁺² ₋₄
QL (UKQCD)	245 \pm 20 ⁺⁰ ₋₂	272 \pm 16 ⁺⁰ ₋₂₀	1.11 \pm 0.03
BS	237	242	1.02
RM	262 \pm 10	298 \pm 11	1.14 \pm 0.09

the delta term is repulsive in this case. It is negligible for higher partial waves due to the centrifugal barrier. However, it is sizable in the 1S_0 channel for which the delta term is attractive.

One expects that the wave functions of the 1^1S_0 and 1^3S_1 states are very similar.⁸¹ In fact, they are equal if the Dirac delta term is ignored. The values with the symbol (\ddagger) in Table 16 are referred to the pseudoscalar decay constants which have been calculated using the wave function of the corresponding 3S_1 state. We recover the agreement with experiment and also with the predictions of different theoretical approaches. The f_{D_s}/f_D and $f_{D_s^*}/f_{D^*}$ ratios are also shown in the last column of Table 16. They are not very sensitive to the delta term and our values agree nicely with experiment and the values obtained in other approaches.

Table 17 summarizes the remaining decay constants needed for the calculation we are interested in. There, we show the results from the constituent quark model in which the 1-loop QCD corrections to the OGE potential and the presence of

Table 17. Decay constants calculated within the CQM including one-loop QCD corrections to the OGE potential and a non- $q\bar{q}$ structure in channel 1^+ .

Meson	f_D (MeV)	$\sqrt{M_D}f_D$ ($\text{GeV}^{3/2}$)
$D_{s0}^*(2317)$	118.706	0.181
$D_{s1}(2460)$	165.097	0.259
$D_{s1}(2536)$	59.176	0.094

Table 18. Ratios of branching fractions for nonleptonic decays $B \rightarrow D^{(*)}D_{sJ}$. The symbol (*) indicates that the ratios have been calculated using the experimental pseudoscalar decay constant in Table 16. For the $D_{s1}(2460)$ and $D_{s1}(2536)$ mesons, the ratios have been calculated without (1) and with (2) taking into account the non- $q\bar{q}$ degrees of freedom in the $J^P = 1^+$ channel.

	$X \equiv D_{s0}^*(2317)$		$X \equiv D_{s1}(2460)$		$X \equiv D_{s1}(2536)$	
	The.	Exp.	The.	Exp.	The.	Exp.
$\mathcal{B}(B \rightarrow DX)/\mathcal{B}(B \rightarrow DD_s)$	0.19(*)	0.10 ± 0.03	-	-	-	-
$\mathcal{B}(B \rightarrow D^*X)/\mathcal{B}(B \rightarrow D^*D_s)$	0.15(*)	0.15 ± 0.06	-	-	-	-
$\mathcal{B}(B \rightarrow DX)/\mathcal{B}(B \rightarrow DD_s^*)$	-	-	$\begin{bmatrix} 0.176^{(1)} \\ 0.177^{(2)} \end{bmatrix}$	0.44 ± 0.11	$\begin{bmatrix} 0.071^{(1)} \\ 0.021^{(2)} \end{bmatrix}$	0.049 ± 0.010
$\mathcal{B}(B \rightarrow D^*X)/\mathcal{B}(B \rightarrow D^*D_s^*)$	-	-	$\begin{bmatrix} 0.251^{(1)} \\ 0.252^{(2)} \end{bmatrix}$	0.58 ± 0.12	$\begin{bmatrix} 0.110^{(1)} \\ 0.032^{(2)} \end{bmatrix}$	0.044 ± 0.010

non- $q\bar{q}$ degrees of freedom in $J^P = 1^+$ charmed-strange meson sector are included. If one compares f_{D_s} ($f_{D_s^*}$) to $f_{D_{s0}^*(2317)}$ ($f_{D_{s1}(2460)}$), one finds that the latter is suppressed.

Our results for the decay constants clearly deviate from the ones obtained in the infinite heavy quark mass limit. In that limit one gets $f_{D_{s0}^*(2317)} = f_{D_s}$, $f_{D_{s1}(2460)} = f_{D_s^*}$ and $f_{D_{s1}(2536)} = 0$, results that lead to a strong disagreement with experiment for the decay width ratios in Eqs. (31) and (32). That was already noticed in Ref. 71, where the authors, using the experimental ratios, estimated that $f_{D_{s0}^*(2317)} \sim \frac{1}{3}f_{D_s}$ and $f_{D_{s0}^*(2317)} \sim f_{D_{s1}(2460)}$ instead. We obtain $f_{D_{s0}^*(2317)}/f_{D_s} = 0.36$, $f_{D_{s0}^*(2317)} \sim 0.72f_{D_{s1}(2460)}$ and $f_{D_{s1}(2536)} = 59.176$ MeV, the latter being small compared to the others but certainly not zero.

Finally, we show in Table 18 our results for the ratios written in Eqs. (31) and (32). The symbol (*) indicates that the ratios have been calculated using the experimental pseudoscalar decay constant in Table 16. We get results close to or within the experimental error bars for the $D_{s0}^*(2317)$ meson, which to us is an indication that this meson could be a canonical $c\bar{s}$ state. The incorporation of the non- $q\bar{q}$ degrees of freedom in the $J^P = 1^+$ channel, enhances the $j_q = 3/2$ component of the $D_{s1}(2536)$ meson and it gives rise to ratios in better agreement

with experiment. Note that the $D_{s1}(2536)$ meson is an almost pure $q\bar{q}$ state in our description.

The situation is more complicated for the $D_{s1}(2460)$ meson. The probability distributions of its 1P_1 and 3P_1 components are corrected by the inclusion of non- $q\bar{q}$ degrees of freedom, the latter making a $\sim 25\%$ of the wave function. In our calculation, only the pure $q\bar{q}$ component of the $D_{s1}(2460)$ meson has been used to evaluate the $\Gamma(B \rightarrow D^{(*)}D_{s1}(2460))$ decay width. The values we get for the corresponding ratios in Eqs. (31) are lower than the experimental data.

7. Summary

A study of heavy meson properties within a nonrelativistic constituent quark model, which successfully describes hadron phenomenology and hadronic reactions, has been presented in this review. Within the heavy quark sector, we have focused on the spectroscopy and on the electromagnetic, strong and weak processes.

An exhaustive study of heavy meson spectra in terms of $q\bar{q}$ components has been performed. The model can be used as a template against which to compare the new mesons, whose nature is still unknown and some of them are in conflict with naive quark model expectations. Some electromagnetic decays have been included. The study of these processes could provide valuable information on the meson structure since the operator of electromagnetic transitions is very well known.

A quite reasonable global description of the charmonium spectra and decay widths has been reached. One striking feature of our model is the new assignment of the $\psi(4415)$ as a D -wave state leaving the $4S$ state for the $X(4360)$. This agrees with the last measurements of its leptonic and total decay widths. We have also tested that our result is compatible with the measured exclusive cross section for the processes $e^+e^- \rightarrow D^0D^-\pi^+$ and $e^+e^- \rightarrow D^0D^{*-}\pi^+$. Tentative assignments of some XYZ mesons as $c\bar{c}$ states have been done.

The situation is more complicate in the open charm and charmed-strange sectors. We describe the charmed and charmed-strange mesons $D^{(*)}$ and $D_s^{(*)}$ and the $j_q^P = \frac{3}{2}^+$ doublet of the orbitally excited states. For the $j_q^P = \frac{1}{2}^+$ doublet the introduction of one loop correction to the OGE potential brings the mass of the 0^+ state closer to experiment but it is not enough to solve the puzzle of these P -wave states.

We have assumed the presence of non- $q\bar{q}$ degrees of freedom in the $J^P = 1^+$ charmed-strange meson sector to enhance the $j_q = 3/2$ component of the $D_{s1}(2536)$ meson. Independently of the mechanism that produces this effect, it has become clear that the description of the $D_{s1}(2536)$ meson as a $j_q = 3/2$ $c\bar{s}$ state is necessary to simultaneously explain its decay properties. The $J^P = 1^+$ $D_{s1}(2460)$ has an important non- $q\bar{q}$ contribution in our framework.

In the last years several new resonances on the open charm sector have been observed. We have discussed their possible quantum numbers attending to their masses and strong decays. We can only partially describe these states, although the

experimental situation is still not clear.

We have also performed a calculation of the branching fractions for the semileptonic decays of B and B_s mesons into final states containing orbitally excited charmed and charmed-strange mesons, respectively. Our results for B semileptonic decays into $D_0^*(2400)$, $D_1(2420)$ and $D_2^*(2460)$ are in good agreement with the latest experimental measurements. In the case of the $D_1(2430)$ meson, the prediction lies a factor of 2 below BaBar. In the case of B_s semileptonic decays, our prediction for the $\mathcal{B}(B_s^0 \rightarrow D_{s1}(2536)^- \mu^+ \nu_\mu) \mathcal{B}(D_{s1}(2536)^- \rightarrow D^{*-} \bar{K}^0)$ product of branching fractions is in agreement with the experimental data. This, together with the strong decay properties studied for the $D_{s1}(2536)$ meson, is to us evidence of a dominant $q\bar{q}$ structure for this state. We have given also predictions for decays into other D_s^{**} mesons which can be useful to test the $q\bar{q}$ nature of these states.

An analysis of the nonleptonic B meson decays into $D^{(*)}D_{sJ}$ has been also included since it provides valuable information about the structure of the $D_{s0}^*(2317)$, $D_{s1}(2460)$ and $D_{s1}(2536)$ mesons. The strong disagreement found between the heavy quark limit predictions and the experimental data is an indication of the finite c -quark mass effects, which are included in the context of the constituent quark model. We have got results close to or within the experimental error bars for the $D_{s0}^*(2317)$ meson, which is an indication that this meson could be a canonical $c\bar{s}$ state. The description of the $D_{s1}(2536)$ meson as an almost 1^+ , $j_q = 3/2$ $c\bar{s}$ state provides theoretical ratios in better agreement with experiment.

To conclude, we have tried to show in this review that many aspects of the charmonium physics can be understood within the framework of the constituent quark model. However there remains interesting open questions which need further theoretical and experimental effort to be clarified.

Acknowledgements

This work has been partially funded by the U.S. Department of Energy, Office of Nuclear Physics, under contract No. DE-AC02-06CH11357. Ministerio de Ciencia y Tecnología under contract No. FPA2010-21750-C02-02 and FIS2011-28853-C02-02, by the European Community-Research Infrastructure Integrating Activity 'Study of Strongly Interacting Matter' (HadronPhysics3 Grant No. 283286), by the Spanish Ingenio-Consolider 2010 Program CPAN (CSD2007-00042).

Bibliography

1. C. Quigg, Quarkonium: New developments, in *The XVIII Rencontres de la Vallée d'Aoste Conference Proceedings*, (2004). FERMILAB-conf-04/033-T, arXiv:hep-ph/0403187v2.
2. R. Galik, Quarkonium production and decay, in *The XXIV Physics in Collisions Conference Proceedings*, (2004). arXiv:hep-ph/0408190.
3. N. Brambilla *et al.*, *The European Physical Journal C - Particles and Fields* **71** (2011) 1.

40 J. Segovia, D.R. Entem, F. Fernandez and E. Hernandez

4. K. K. Seth, New results from cleo and bes, in *Journal of Physics: Conference Series*, (2005), p. 32.
5. K. K. Seth, Heavy Quarkonia Results from CLEO, in *Nuclear Physics B: Proceedings Supplements*, (2005), p. 344.
6. K. Seth *et al.*, Heavy Quarkonia—A review of the experimental status, in *Nuclear Physics B: Proceedings Supplements*, (1) (2006), p. 207.
7. T. Skwarnicki, Cleo results on transitions in heavy quarkonia, in *The 40th Rencontres De Moriond On QCD And High Energy Hadronic Interactions Conference Proceedings*, (2005). arXiv:hep-ex/0505050.
8. E. Eichten, K. Gottfried, T. Kinoshita, K. D. Lane and T. M. Yan, *Phys. Rev. D* **17** (1978) 3090.
9. S. F. Radford and W. W. Repko, *Phys. Rev. D* **75** (2007) 074031.
10. N. Isgur and G. Karl, *Phys. Rev. D* **19** (1979) 2653.
11. N. Isgur, *International Journal of Modern Physics E* **01** (1992) 465.
12. A. Manohar and H. Georgi, *Nuclear Physics B* **234** (1984) 189 .
13. D. Dyakonov and V. Petrov, *Nuclear Physics B* **272** (1986) 457 .
14. S. N. Gupta and S. F. Radford, *Phys. Rev. D* **24** (1981) 2309.
15. E. Hiyama, Y. Kino and M. Kamimura, *Prog. Part. Nucl. Phys.* **51** (2003) 223.
16. J. Segovia, A. M. Yasser, D. R. Entem and F. Fernández, *Phys. Rev. D* **78** (2008) 114033.
17. J. Beringer *et al.*, *Phys. Rev. D* **86** (2012) 010001.
18. S. Godfrey and N. Isgur, *Phys. Rev. D* **32** (Jul 1985) 189.
19. D. Ebert, R. Faustov and V. Galkin, *Eur. Phys. J.* **C71** (2011) 1825.
20. Belle Collaboration (S. Uehara *et al.*), *Phys. Rev. Lett.* **104** (2010) 092001.
21. Belle Collaboration (X. L. Wang *et al.*), *Phys. Rev. Lett.* **99** (2007) 142002.
22. Belle Collaboration (G. Pakhlova *et al.*), *Phys. Rev. Lett.* **101** (2008) 172001.
23. Belle Collaboration (S. Uehara *et al.*), *Phys. Rev. Lett.* **96** (2006) 082003.
24. Belle Collaboration (V. Bhardwaj *et al.*), *arXiv:hep-ex/1304.3975* (2013).
25. Belle Collaboration (S.-K. Choi *et al.*), *Phys. Rev. Lett.* **89** (2002) 102001.
26. CLEO Collaboration (S. Dobbs *et al.*), *Phys. Rev. Lett.* **101** (2008) 182003.
27. BESIII Collaboration (M. Ablikim *et al.*), *Phys. Rev. Lett.* **104** (2010) 132002, $\Gamma = 0.73 \pm 0.45 \pm 0.28$ and $\mathcal{B} = (54.3 \pm 6.7 \pm 5.2) \times 10^{-2}$.
28. P. G. Ortega, J. Segovia, D. R. Entem and F. Fernández, *Phys. Rev. D* **81** (2010) 054023.
29. Belle Collaboration (S.-K. Choi *et al.*), *Phys. Rev. Lett.* **94** (2005) 182002.
30. BaBar Collaboration (B. Aubert *et al.*), *Phys. Rev. Lett.* **101** (2008) 082001.
31. J. J. Dudek, R. G. Edwards and C. E. Thomas, *Phys. Rev. D* **79** (May 2009) 094504.
32. BaBar Collaboration (P. del Amo Sanchez *et al.*), *Phys. Rev. D* **82** (2010) 111101.
33. LHCb collaboration Collaboration (R. Aaij *et al.*) (2013) arXiv:1307.4556 [hep-ex].
34. BaBar Collaboration (B. Aubert *et al.*), *Phys. Rev. D* **80** (2009) 092003.
35. LHCb Collaboration Collaboration (R. Aaij *et al.*), *JHEP* **1210** (2012) 151, arXiv:1207.6016 [hep-ex].
36. D. Ebert, R. Faustov and V. Galkin, *Eur. Phys. J.* **C66** (2010) 197.
37. M. Di Pierro and E. Eichten, *Phys. Rev. D* **64** (Oct 2001) 114004.
38. G. S. Bali, *Phys. Rev. D* **68** (2003) 071501.
39. O. Lakhina and E. S. Swanson, *Physics Letters B* **650** (2007) 159.
40. A. Badalian, B. Ioffe and A. V. Smilga, *Nucl. Phys.* **B281** (1987) 85.
41. M. Ablikim *et al.*, *Physics Letters B* **660** (2008) 315.
42. CLEO Collaboration (M. Artuso *et al.*), *Phys. Rev. D* **80** (2009) 112003.
43. CLEO Collaboration (H. Mendez *et al.*), *Phys. Rev. D* **78** (2008) 011102.

44. L. Micu, *Nucl. Phys.* **B10** (1969) 521.
45. A. Le Yaouanc, L. Oliver, O. Pène and J. C. Raynal, *Phys. Rev. D* **8** (1973) 2223.
46. A. Le Yaouanc, L. Oliver, O. Pène and J.-C. Raynal, *Phys. Rev. D* **9** (1974) 1415.
47. J. Segovia, D. Entem and F. Fernandez, *Phys.Lett.* **B715** (2012) 322.
48. K. K. Seth, *Phys. Rev. D* **72** (2005) 017501.
49. B. Aubert, A precision measurement of the d_s1 (2536) meson mass and decay width, in *33rd International Conference on High-Energy Physics*, (2006). arXiv:hep-ex/0607084.
50. P. Colangelo, F. De Fazio, F. Giannuzzi and S. Nicotri, *Phys. Rev. D* **86** (2012) 054024.
51. Belle Collaboration (V. Balagura *et al.*), *Phys. Rev. D* **77** (2008) 032001.
52. J. Vijande, F. Fernández and A. Valcarce, *Phys. Rev. D* **73** (2006) 034002.
53. Belle Collaboration (G. Pakhlova *et al.*), *Phys. Rev. Lett.* **100** (2008) 062001.
54. Belle Collaboration (G. Pakhlova *et al.*), *Phys. Rev. D* **80** (2009) 091101.
55. Gerson, S. Goldhaber, A. Barbaro-Galtieri *et al.*, *Advances in Particle Physics*, vol. 2, p. 197 (Cool, Marshak Eds., 1968).
56. J. M. Blatt and V. F. Weisskopf, *Theoretical nuclear physics* (Dover Pubns, 1991).
57. T. Barnes, S. Godfrey and E. S. Swanson, *Phys. Rev. D* **72** (2005) 054026.
58. Belle Collaboration (D. Liventsev *et al.*), *Phys. Rev. D* **77** (2008) 091503.
59. BaBar Collaboration (B. Aubert *et al.*), *Phys. Rev. Lett.* **101** (2008) 261802.
60. BaBar Collaboration (B. Aubert *et al.*), *Phys. Rev. Lett.* **103** (2009) 051803.
61. D0 Collaboration (V. M. Abazov *et al.*), *Phys. Rev. Lett.* **102** (2009) 051801.
62. M. A. Ivanov, J. G. Körner and P. Santorelli, *Phys. Rev. D* **73** (2006) 054024.
63. E. Hernández, J. Nieves and J. M. Verde-Velasco, *Phys. Rev. D* **74** (2006) 074008.
64. J. Segovia, C. Albertus, D. R. Entem, F. Fernández, E. Hernández and M. A. Perez-Garcia, *Phys. Rev. D* **84** (2011) 094029.
65. Belle Collaboration (P. Krokovny *et al.*), *Phys. Rev. Lett.* **91** (2003) 262002.
66. BaBar Collaboration (B. Aubert *et al.*), *Phys. Rev. D* **74** (2006) 091101.
67. BaBar Collaboration (B. Aubert *et al.*), *Phys. Rev. D* **77** (2008) 011102.
68. Belle Collaboration (J. Dalseno *et al.*), *Phys. Rev. D* **76** (2007) 072004.
69. Belle Collaboration (T. Aushev *et al.*), *Phys. Rev. D* **83** (2011) 051102.
70. A. L. Yaouanc, L. Oliver, O. Pène and J.-C. Raynal, *Physics Letters B* **387** (1996) 582.
71. A. Datta and P. O'Donnell, *Physics Letters B* **572** (2003) 164.
72. A. L. Yaouanc, L. Oliver, O. Pène, J.-C. Raynal and V. Morénas, *Physics Letters B* **520** (2001) 59 .
73. P. Colangelo and F. D. Fazio, *Physics Letters B* **532** (2002) 193.
74. P. Colangelo, F. De Fazio, G. Nardulli, N. Paver and Riazuddin, *Phys. Rev. D* **60** (1999) 033002.
75. Z. Luo and J. L. Rosner, *Phys. Rev. D* **64** (2001) 094001.
76. A. Abd El-Hady, A. Datta and J. P. Vary, *Phys. Rev. D* **58** (1998) 014007.
77. A. Abd El-Hady, A. Datta, K. S. Gupta and J. P. Vary, *Phys. Rev. D* **55** (1997) 6780.
78. F. Jugeau, A. Le Yaouanc, L. Oliver and J.-C. Raynal, *Phys. Rev. D* **72** (2005) 094010.
79. J. Segovia, C. Albertus, E. Hernández, F. Fernández and D. R. Entem, *Phys. Rev. D* **86** (2012) 014010.
80. Guo-Li and Wang, *Physics Letters B* **633** (2006) 492.
81. M.B. and Voloshin, *Progress in Particle and Nuclear Physics* **61** (2008) 455.